Original Article

Machine learning improves risk stratification of coronary heart disease and stroke

Bangwei Chen[1,2,3#^], Lei Ruan[4#], Liuqiao Yang[2,3,5#], Yucong Zhang[4], Yueqi Lu[2,3], Yu Sang[4], Xin Jin[2,3], Yong Bai[2,3], Cuntai Zhang[4], Tao Li[2,3]

[1]School of Biology and Biological Engineering, South China University of Technology, Guangzhou, China; [2]BGI-Shenzhen, Shenzhen, China; [3]China National GeneBank, Shenzhen, China; [4]Department of Geriatrics, Tongji Hospital, Tongji Medical College, Huazhong University of Science and Technology, Wuhan, China; [5]College of Life Sciences, University of Chinese Academy of Sciences, Beijing, China

Contributions: (I) Conception and design: T Li, C Zhang, Y Bai; (II) Administrative support: X Jin; (III) Provision of study materials or patients: Y Sang, Y Zhang, L Ruan; (IV) Collection and assembly of data: Y Sang, Y Zhang, L Ruan; (V) Data analysis and interpretation: B Chen, Y Bai, L Yang, Y Lu; (VI) Manuscript writing: All authors; (VII) Final approval of manuscript: All authors.

[#]These authors contributed equally to this work.

Correspondence to: Cuntai Zhang. Department of Geriatrics, Tongji Hospital, Tongji Medical College, Huazhong University of Science and Technology, 1095 Jiefang Avenue, Wuhan 430030, China. Email: ctzhang0425@163.com; Tao Li. BGI-Shenzhen, Building 11, Beishan Industrial Zone, Yantian District, Shenzhen 518083, China. Email: litao2@genomics.cn.

Background: Coronary heart disease (CHD) and cerebral ischemic stroke (CIS) are two major types of cardiovascular disease (CVD) that are increasingly exerting pressure on the healthcare system worldwide. Machine learning holds great promise for improving the accuracy of disease prediction and risk stratification in CVD. However, there is currently no clinically applicable risk stratification model for the Asian population. This study developed a machine learning-based CHD and CIS model to address this issue.

Methods: A case-control study was conducted based on 8,624 electronic medical records from 2008 to 2019 at the Tongji Hospital in Wuhan, China. Two machine learning methods (the random down-sampling method and the random forest method) were integrated into 2 ensemble models (the CHD model and the CIS model). The trained models were then interpreted using Shapley Additive exPlanations (SHAP).

Results: The CHD and CIS models achieved good performance with the areas under the receiver operating characteristic curve (AUC) of 0.895 and 0.884 in random testing, and 0.905 and 0.889 in sequential testing, respectively. We identified 4 common factors between CHD and CIS: age, brachial-ankle pulse wave velocity, hypertension, and low-density lipoprotein cholesterol (LDL-C). Moreover, carcinoembryonic antigen (CEA) was identified as an independent indicator for CHD.

Conclusions: Our ensemble models can provide risk stratification for CHD and CIS with clinically applicable performance. By interpreting the trained models, we provided insights into the common and unique indicators in CHD and CIS. These findings may contribute to a better understanding and management of risk factors associated with CVD.

Keywords: Coronary heart disease (CHD); ischemic stroke; machine learning; risk stratification

Submitted Apr 12, 2022. Accepted for publication Sep 05, 2022.
doi: 10.21037/atm-22-1916
View this article at: https://dx.doi.org/10.21037/atm-22-1916

^ ORCID: 0000-0003-4348-2938.

Introduction

Cardiovascular diseases (CVDs) are a leading cause of global mortality and morbidity. In China, 93.8 million CVD patients were reported in 2016, more than twice the number reported in 1990 (40.6 million) (1). By 2019, cardiovascular death accounted for 45.19% of total deaths in rural areas and 43.56% in urban areas. The incessant increase in CVD prevalence has been highlighted as a global health challenge (2). Therefore, improving the efficiency of the CVD healthcare system is an urgent task.

It is now widely accepted that machine learning can improve medical efficiency by assisting doctors in analyzing large-scale high-dimensional clinical data. The merit of machine learning has been consistently supported by several predictive and risk stratification studies (3), including those for CVD and its subtypes (4,5). Notably, an effective stroke classification model was trained using a Chinese prospective cohort with 56 stroke patients and 1,075 non-stroke participants. This study applied a synthetic minority over-sampling technique (SMOTE) method for data balancing, which achieved an area under the receiver operating characteristic curve (AUC) of 0.72 (6). It should be noted that CVD patients appear relatively rarely in the natural population, which highlights the potential imbalance issues in model training. Early risk assessment may prevent cardiovascular events in the future (7). In clinical practice, people often have poor compliance (8) and it may be difficult to identify people at high risk of CVD. Therefore, an efficient risk stratification model is necessary. Furthermore, the Asian population is underrepresented in published studies. As illustrated in Liu's research, the models based on the European population may overestimate the risk in Asian populations (9). To address the problems of imbalance and population difference, we integrated the machine learning models with the under-sampling method to create a coronary heart disease (CHD) and cerebral ischemic stroke (CIS) risk stratification model that is clinically applicable for the Asian population. We present the following article in accordance with the TRIPOD reporting checklist (available at https://atm.amegroups.com/article/view/10.21037/atm-22-1916/rc).

Methods

Study design

A case-control study was conducted with participants attending a physical examination at Tongji Hospital in Wuhan, China, from May 2008 to December 2019. The inclusion criteria were as follows: (I) patients aged 30 years and older; and (II) patients without a history of tumor, liver cirrhosis, or renal failure. Participants with a recorded CHD or CIS history were considered cases. Participants without any history of CHD and CIS were considered controls.

The study was conducted in accordance with the Declaration of Helsinki (as revised in 2013). The study was approved by the Medical Ethics Committee at Tongji Medical College, Huazhong University of Science and Technology (No. TJ-IRB20191215). Individual consent for this retrospective analysis was waived.

Clinical indicators and inclusion criteria

The medical records of all the participants were collated at the Tongji Hospital during standardized in-person interviews (10). A total of 118 indicators were selected from medical records, including lifestyle characteristics and clinical measurements. The standardized protocols of data collection can be found in the Supplementary Methods (Appendix 1).

The diagnosis of CIS was based on symptoms and cerebral infarction confirmed by computed tomography or magnetic resonance imaging; CHD was diagnosed according to symptoms (mainly angina) and electrocardiography or coronary angiography. Patients with self-reported CHD, coronary artery bypass grafting, coronary stent implantation, percutaneous coronary intervention, or percutaneous transluminal coronary angioplasty were also considered CHD patients. The patient's self-reports were confirmed by doctors through the medical insurance system.

Imputation

Indicators with a missing rate greater than 45% were discarded, and the remaining missing indicators were imputed (Table S1). Random forest was applied to impute the missing continuous data with the R package missForest v1.4 (11). Missing categorical data were imputed by the median of each feature.

Model establishment

CHD and CIS datasets were built to train the CHD and CIS models. The unreliable data were excluded, defined by inconsistency in gender, age (differences larger than 5 years), or physical examination time with cases.

In each dataset, 80% of the data before 1 January 2018 were randomly sampled as the training set, and the remaining 20% were used for random testing. The data collected after the year 2018 were used for sequential testing.

All continuous variables were standardized with a mean of 0 and a variance of 1. Three feature selection approaches were applied for continuous features: (I) analysis of variance (ANOVA) (12); (II) recursive feature elimination (RFE) (13); and (III) Boruta (14). The P value threshold of ANOVA was set at 0.05. The basic estimator of both RFE and Boruta was a random forest model with default parameters (15). Continuous features significant in at least two methods were selected for subsequent analysis.

For categorical features, the VarianceThreshold method was used to exclude the features that were either 1 or 0 in more than 80% of the samples. All feature selection methods were performed in Python 3.7 using the packages sklearn v0.24 and Boruta v0.3 (14,16).

A bagging classifier was developed with additional balancing from BalancedBaggingClassifier using the python package scikit-multilearn v0.2 (17). Specifically, the base estimator was the random forest model (15). Random down-sampling without replacement was used to produce a more balanced dataset. The ratio of major classes to minor classes was 1, and the number of downsampling (number of base models) was 100. The training process included hyper-parameters selection and model simplification. The hyper-parameters (n_estimators, max_depth, and min_samples_split) were searched to maximize the AUC score using GridSearchCV in 5-fold cross-validation. To improve the efficiency in clinical practice, an approach was applied to reduce the number of indicators while ensuring the utility of the risk stratification model. The Shapley Additive exPlanations (SHAP) explainer (18) was constructed to rank the features using Python package shap v0.39, and 1,000 randomly selected samples were used to calculate the feature contribution. We used 80% of the randomly selected sets to train a model, and the remaining 20% of the samples were used for model evaluation. The features with a higher ranking were included unless no improvements were observed. The above training and validation process was repeated 100 times to secure robustness. Measures (average precision, specificity, sensitivity, F-score, and AUC) were used to systematically evaluate the performance. The trained model was interpreted by SHAP.

To better evaluate the performance of the final model, the complex model before reducing feature numbers, random forest model, logistic regression model, and support vector machine model was constructed. Constructions of the above three traditional machine learning models used the same characteristics as the complex model. Framingham risk scores (FHS) of CHD and CIS were calculated. The risk prediction equations of CHD (19) and CIS (20) for 10 years are presented in Supplementary Methods.

Development of risk stratification Python package

A Python package named CCRS (coronary heart disease and cerebral ischemic stroke risk stratification) was developed for generating better application in clinics by providing population risk and relative risk. Population risk would be categorized into mild, moderate, and severe. In detail, based on CHD and CIS models' prediction in the training data, the threshold between mild and moderate corresponded to the true positive rate of 95%, and the threshold between severe and moderate corresponded to the true negative rate of 95%. The relative risk would be presented as risk ranking among peers. For the purpose of clarity, with the individual predicted value and age, the ranking of the individuals in the same age group of the training set was provided as relative risk.

Statistical analysis

Continuous variables were presented as means and standard deviations. Categorical variables were described as counts and percentages. To evaluate the difference between case and control groups, continuous indicators were analyzed by the rank sum test and categorical indicators were analyzed by the chi-square test. Delong methods were used to test the differences in the AUCs of the receiver operating characteristic (ROC) curves.

Results

Basic characteristics of the study population

This study included 7,983 (92.6%) controls and 641 (7.4%) cases (*Figure 1*). Among the cases, 302 were CHD patients and 302 were CIS patients, and 37 people had both CHD and CIS. The mean age of the study population was 51±11.4 years and 71.3% of the study population were males.

All 118 clinical indicators are presented in Table S2. The lifestyle characteristics and laboratory results relevant to blood pressure, glucose, and lipids are summarized in *Table 1*.

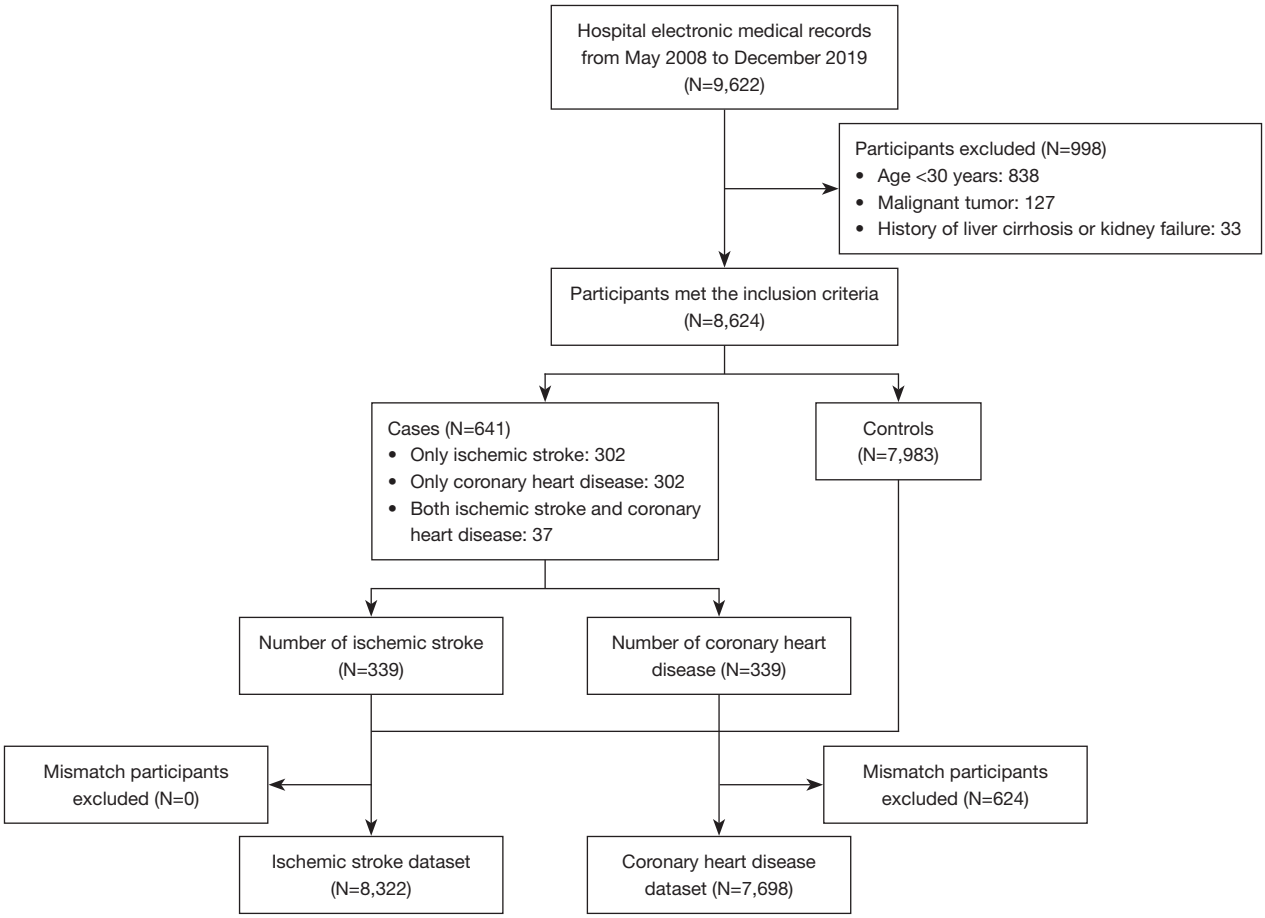

Figure 1 A flowchart depicting the study process.

The proportion of smokers and drinkers in the study population was 32.2% and 44.3%, respectively. In terms of vascular stiffness, 99.2% of the population had normal ankle-brachial index (ABI; 0.9≤ ABI <1.4) (21), and 55.7% of the population had normal brachial-ankle pulse wave velocity (baPWV <1,400) (22). These characteristics in the CHD dataset (N=7,698) and CIS dataset (N=8,322) are presented in Table S3 and Table S4.

The ensemble learning model effectively distinguished CHD patients and CIS patients

The flowchart of model development is shown in *Figure 2*. After standardization, the first step of training was the elimination of irrelevant and redundant information. In this step, VarianceThreshold, ANOVA, RFE, and Boruta were used for features selection. After selection, only 5 of the 55 discrete variables presented significant contribution in both CHD and CIS patients, namely, sex, smoking status, drinking, vascular stiffness, and hypertension. Meanwhile, 23 of the 59 continuous variables were considered important in the CHD dataset, and 22 of the 59 variables showed importance in the CIS dataset (Table S4). Five features, namely, age, prostate-specific antigen (PSA), total cholesterol (TC), baPWV, and estimated glomerular filtration rate (eGFR), were considered crucial in both CHD and CIS patients (Figure S1, Table S5).

GridSearchCV analysis was then applied to optimize the balanced bagging classifier (BBC) model. The optimal hyper-parameters for the optimal CHD classification performance were as follows: estimators 100, maximum depth 6, and minimum sample split 7 (Figure S2). In terms of the CIS model, the ideal hyper-parameters were as follows: estimators 500, maximum depth 4, and minimum sample split 2 (Figure S3).

We then used SHAP analysis to reduce the model

Table 1 Basic characteristics of the study population

Variables	Population (N=8,624)
Basic characteristics	
Age, years	51.9±11.4
Sex	
Male	6,152 (71.3)
Female	2,472 (28.7)
Smoker	2,777 (32.2)
Drinker	3,823 (44.3)
BMI, kg/m^2	24.6±3.1
Cardiovascular medical history	
CHD	339 (3.9)
CIS	339 (3.9)
Clinical measurements	
SBP, mmHg	126.3±16.9
DBP, mmHg	81.7±11.4
LDL-C, mmol/L	2.9±0.8
HDL-C, mmol/L	1.2±0.3
TC, mmol/L	4.7±0.9
TG, mmol/L	1.6±1.4
FBG, mmol/L	5.2±1.2
HbA1c, %	5.8±0.7
baPWV, cm/s	1,409.7±256.5
<1,400	4,800 (55.7)
1,400–1,800	3,191 (37.0)
>1,800	633 (7.3)
ABI	1.1±0.07
<0.9	59 (0.7)
0.9–1.4	8,554 (99.2)
>1.4	11 (0.1)

Continuous variables are described as mean ± SD. Categorical variables are described as number (percentage). BMI, body mass index; CHD, coronary heart disease; CIS, cerebral ischemic stroke; SBP, systolic blood pressure; DBP, diastolic blood pressure; LDL-C, low-density lipoprotein cholesterol; HDL-C, high-density lipoprotein cholesterol; TC, total cholesterol; TG, triglyceride; FBG, fasting blood glucose; HbA1c, hemoglobin A1C; baPWV, brachial-ankle pulse wave velocity; ABI, ankle-brachial index; SD, standard deviation.

complexity. The CHD model performance was retained when including the top 8 features (Figure S4). For the CIS model, only 5 features were required for maintaining the model efficiency (Figure S5). Lastly, the final ensemble models were built based on the optimized parameters and features.

To evaluate the model performance, multiple reported models were constructed, including Framingham risk score (19,20), BBC model before reducing feature numbers, and traditional machine learning models (logistic regression, support vector machine, and random forest), by applying multiple measures. These measures included ROC curves, sensitivity, specificity, F score, and average precision. In the CHD model, the AUCs of the random and the sequential validation were 0.895 and 0.905, respectively (*Figure 3A*). The area under the precision-recall curves (AUPRCs) of the random and the sequential validation was 0.360 and 0.304, respectively (*Figure 3B*). The sensitivity of the random and the sequential validation was 0.807 and 0.873, and the specificity was 0.831 and 0.788, respectively (*Table 2*). Compared with other models horizontally, the model with the best performance was the BBC model before simplification, and the final BBC model performed similarly to that of the complex BBC model in the sequential test set (Figure S6). In the CIS model, the AUCs of the random and the sequential test set were 0.884 and 0.889, respectively (*Figure 3C*). The AUPRCs of the random and the sequential validation were 0.298 and 0.216, respectively (*Figure 3D*). The sensitivity of the random and the sequential validation was 0.808 and 0.877, and the specificity was 0.750 and 0.756, respectively (*Table 3*). Interestingly, the performance of the final model was superior to that of other CIS models horizontally (Figure S7). Notably, in both models, the predictive performance of the sequential validation was better than those of the random validation. Considering that the AUC can only reflect the discrimination of the models, the calibration of the models was evaluated (Figure S8). Unfortunately, the calibration of the models was generally poor and the BBC models for CHD and CIS might overestimate the risk.

Model interpretation

We applied SHAP analysis to interpret and understand the mechanism underlying the trained model. Our results indicated that hypertension, increased age, baPWV,

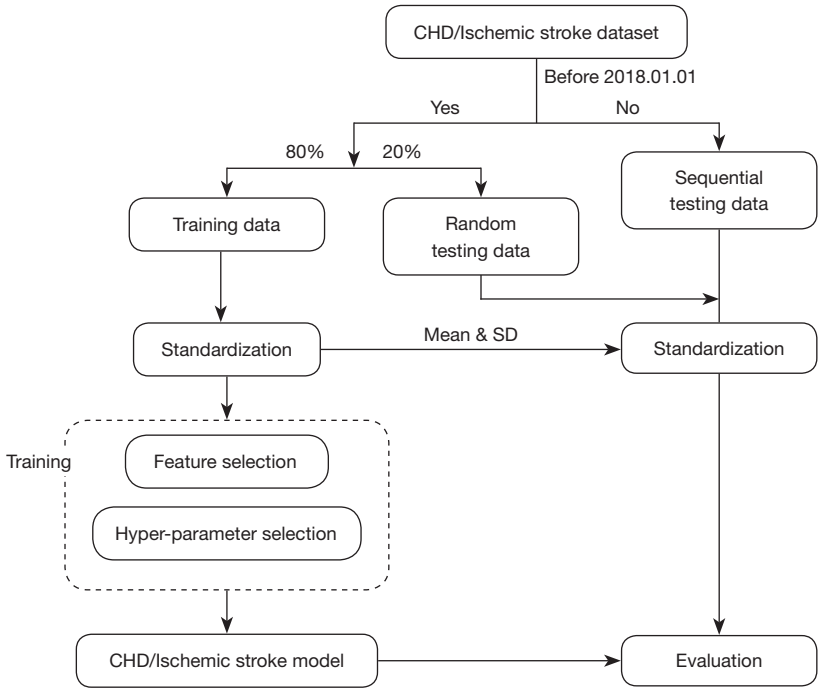

Figure 2 Training and validation of the model. CHD, coronary heart disease; SD, standard deviation.

hemoglobin A1c (HbA1c), and carcinoembryonic antigen (CEA) were associated with a higher risk of CHD. Meanwhile, high levels of TC, low-density lipoprotein cholesterol (LDL-C), and platelet (PLT) were associated with a lower risk of CHD (*Figure 4A*,*4B*). An increase in LDL-C was negatively correlated with the risk of CIS, and hypertension, increased age, baPWV, and ABI were positively correlated with the risk of CIS (*Figure 4C*,*4D*). In both diseases, hypertension appeared to be a common risk factor. In addition, the effects of continuous variables were linear (Spearman correlation, P<0.001, Figures S9,S10). Intriguingly, in the CHD model, the impact of CEA failed to enhance when the value was greater than 3.14. In the CIS model, the impact of ABI steeply increased when its value was greater than 1.1 (*Figure 4E*). In addition, the effect of age presented an S-curve in both models. To further explore the characteristics of the CEA influence curve, interaction analysis was used. The results showed that the SHAP value of CEA in individuals with high levels of LDL-C was higher in the plateau stage (*Figure 4F*).

Although the feature selection process excluded the feature of gender, gender differences have been observed in CVD (23) We suspected that the effects of some other features may vary in different gender groups, which was supported by the sex-specific sub-analysis, where hypertension remained an important predictor of CHD and CIS in males, but the importance decreased in females. Other features such as age and baPWV appeared to be critical predictors in both males and females (Figure S11).

Inflammation status could be essential in CVD development

For in-depth study, the misclassifications in our model predicted accurate samples and predicted wrong controls (PWCs) were used for error analysis. The results demonstrated that the PWCs were similar to the predicted accurate patients (PAP; P>0.05), but different from the predicted accurate controls (PACs) in age, baPWV, HbA1c, CEA, and PLT (Figure S12A-S12E, P<0.001).

However, the percentage of lymphocytes in PWCs (33.0±7.9) was close to that in PACs (33.5±7.3, P=0.27) and was higher than that in PAP samples (27.2±7.4, P=0.01, Figure S12F). Considering that leukocytes are related to immunity and inflammation, we further analyzed the neutrophil count, neutrophil/lymphocyte ratio (NLR), and systemic immune inflammation index (SII) of PWCs without antiplatelet medication (*Table 4*). The SII in PWCs (361.9±170.4) was not only lower than that in PAPs (525.1±305.0, P<0.001), but also lower than that found in

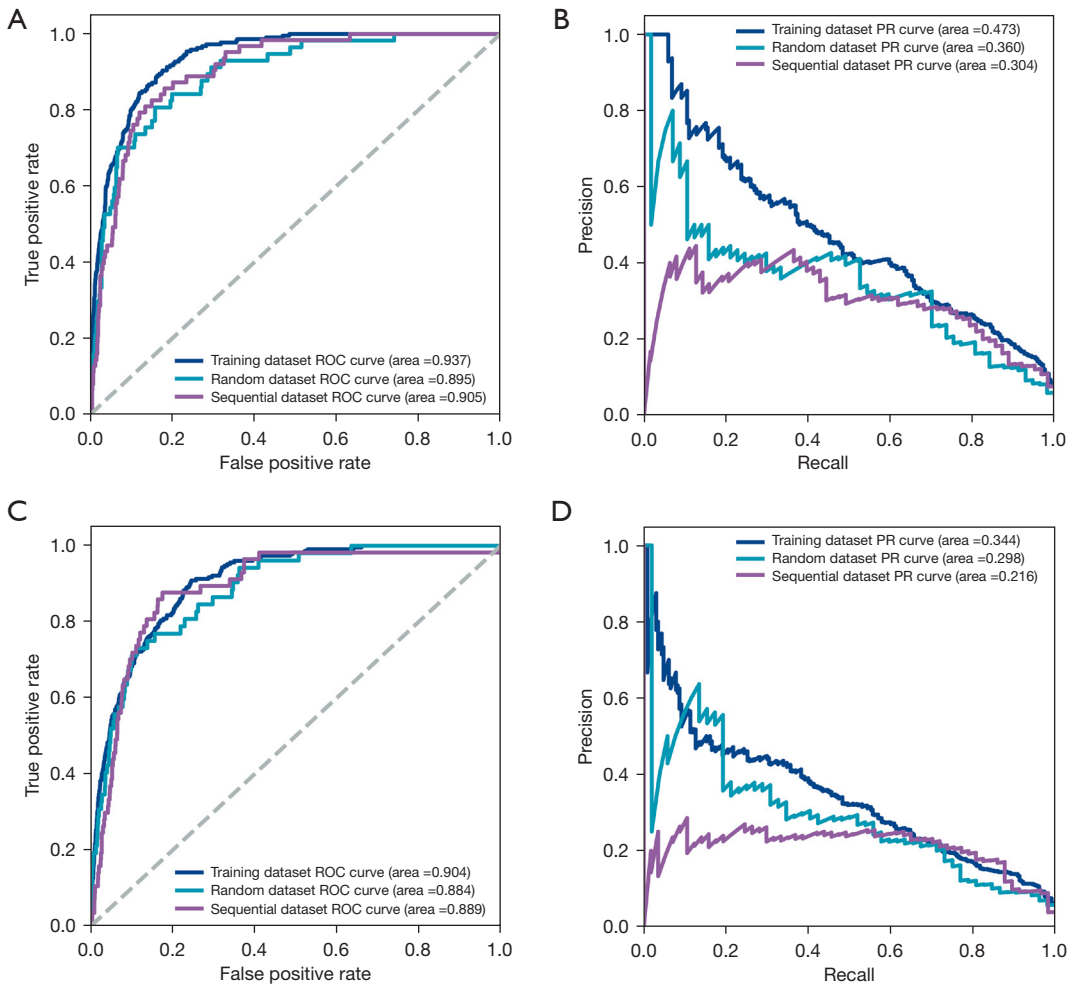

Figure 3 Evaluation of the models. (A) ROC analysis was applied to calculate the AUC, which was used to assess the performance of the CHD model in training, random, and sequential testing. (B) The precision and recall curve of the CHD model in training, random, and sequential testing. (C) ROC analysis was used to calculate AUC, which was used to evaluate the performance of the CIS model in training, random, and sequential testing. (D) The precision and recall curve of the CIS model in training, random, and sequential testing. ROC, receiver operating characteristic; PR, precision and recall; AUC, area under the receiver operating characteristic curve; CHD, coronary heart disease; CIS, cerebral ischemic stroke.

PACs (420.8±189.9, P<0.001, *Table 5*, Figure S13). The error analysis revealed that the PWCs were comparable to the PAPs in all 5 indicators, but different from the PACs (P<0.001) in the CIS model. Unfortunately, error analysis could not be performed in predicted wrong cases due to the limited sample size.

The constructed model achieved precise risk stratification in CVD

When applying the risk stratification model to the sequential testing dataset, 93.8% of CHD patients and 95.0% of CIS patients were classified into the moderate or severe group (*Figure 5A*,*5B*). The risk stratification model was used to calculate the relative risk of participants in each age group. The relative risk of CHD and CIS patients was higher than that in controls for each age group (one-sided rank-sum test P<0.001, *Figure 5C*,*5D*).

Discussion

In this study, an effective model for risk stratification in

Table 2 Evaluation scores for the CHD model

Models	AUC (95% CI)	Specificity	Sensitivity	F-score	AP
Random testing					
FHS-CHD	0.708 (0.65–0.762)	0.545	0.737	0.128	0.063
LR	0.901 (0.868–0.933)	0.836	0.807*	0.303	0.159
SVM	0.874 (0.829–0.915)	0.829	0.772	0.283	0.144
RF	0.899 (0.866–0.929)	0.815	0.789	0.274	0.140
Complex BBC	0.912 (0.884–0.937)*	0.868*	0.789	0.341*	0.181*
BBC	0.895 (0.860–0.928)	0.831	0.807*	0.297	0.155
Sequential testing					
FHS-CHD	0.73 (0.683–0.779)	0.570	0.794	0.157	0.080
LR	0.900 (0.870–0.927)	0.807	0.857	0.308	0.168
SVM	0.877 (0.841–0.909)	0.806	0.794	0.287	0.149
RF	0.903 (0.872–0.932)	0.774	0.905*	0.289	0.160
Complex BBC	0.905 (0.876–0.931)*	0.827*	0.841	0.325*	0.177*
BBC	0.905 (0.877–0.931)*	0.788	0.873	0.293	0.160

*, the highest scores in random testing or sequential testing. CHD, coronary heart disease; AUC, the area under the receiver operating characteristic curve; CI, confidence interval; AP, average precision; FHS-CHD, Framingham risk score of coronary heart disease; LR, logistic regression; SVM, support vector machine; RF, random forest; BBC, balanced bagging classifier.

Table 3 The evaluation scores for the CIS model

Models	AUC (95% CI)	Specificity	Sensitivity	F-score	AP
Random testing					
FHS-CIS	0.804 (0.757–0.851)	0.791	0.596	0.172	0.075
LR	0.882 (0.848–0.913)	0.748	0.885*	0.213	0.112
SVM	0.839 (0.793–0.883)	0.776	0.808	0.215	0.107
RF	0.865 (0.821–0.909)	0.842*	0.750	0.260*	0.127*
Complex BBC	0.880 (0.843–0.916)	0.780	0.808	0.218	0.109
BBC	0.884 (0.850–0.919)*	0.750	0.808	0.198	0.098
Sequential testing					
FHS-CIS	0.850 (0.812–0.886)	0.815	0.719	0.232	0.110
LR	0.883 (0.847–0.912)	0.779	0.825	0.229	0.117
SVM	0.813 (0.762–0.857)	0.784	0.754	0.215	0.104
RF	0.872 (0.827–0.912)	0.827*	0.807	0.268*	0.137*
Complex BBC	0.877 (0.836–0.914)	0.787	0.877*	0.249	0.132
BBC	0.889 (0.851–0.919)*	0.756	0.877*	0.225	0.118

*, the highest scores in random testing or sequential testing. CIS, cerebral ischemic stroke; AUC, the area under the receiver operating characteristic curve; CI, confidence interval; AP, average precision; FHS-CIS, Framingham risk score of cerebral ischemic stroke; LR, logistic regression; SVM, support vector machine; RF, random forest; BBC, balanced bagging classifier.

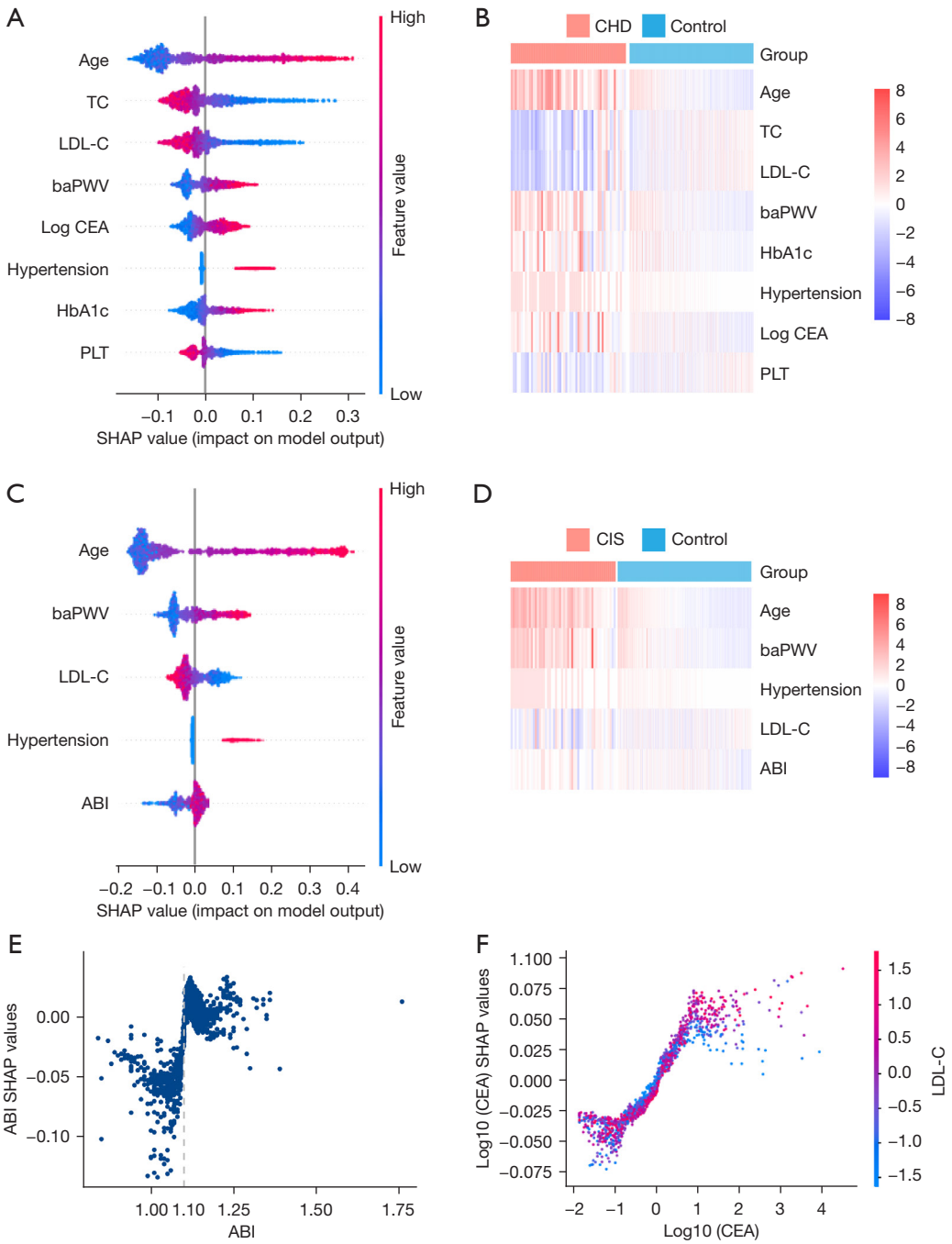

Figure 4 Model interpretation through SHAP analysis. (A) An overview the feature impact on the CHD model. Dots represented SHAP values of every feature for each sample. Colors represented the feature value (red: high value, blue: low value). (B) A heatmap showing the feature values in the CHD dataset. (C) An overview of the feature impact on the CIS model. Dots represented SHAP values of every feature for each sample. Colors represented the feature value (red: high value, blue: low value). (D) A heatmap showing the feature values in the CIS dataset. (E) The SHAP values changed in predicted CIS as ABI. (F) The SHAP values changed in predicted CHD as CEA. Vertical dispersion at a single value of CEA represents the interaction strength with LDL-C. The color represents the LDL-C value. TC, total cholesterol; LDL-C, low density lipoprotein cholesterol; baPWV, brachial-ankle pulse wave velocity; CEA, carcinoembryonic antigen; HbA1c, hemoglobin A1c; PLT, platelet; CHD, coronary heart disease; ABI, ankle-brachial index; CIS, cerebral ischemic stroke; SHAP, Shapley Additive exPlanations.

Table 4 Use of antiplatelet drugs in CHD patients

Use of antiplatelet drugs	Predicted accurate cases	Predicted accurate controls	Predicted wrong controls
Yes	33	8	14
No	21	987	206

CHD, coronary heart disease.

Table 5 Statistical test results (P values) of inflammatory markers in the CHD dataset

Inflammatory indicators	PAC *vs.* PWC	PAP *vs.* PWC	PAC *vs.* PAP
Neutrophils	0.602	2.75×10^{-2}	3.61×10^{-2}
NLR	0.711	4.30×10^{-3}	1.40×10^{-3}
SII	7.27×10^{-6}	5.35×10^{-3}	0.118

CHD, coronary heart disease; PAC, predicted accurate controls; PWC, predicted wrong controls; PAP, predicted accurate patients; NLR, neutrophil/lymphocyte ratio; SII, systemic immune inflammation index, SII was calculated by (N×P)/L (N, P, and L represent neutrophil counts, platelet counts, and lymphocyte counts, respectively).

CHD and CIS was developed based on 8,624 electronic medical records among the Chinese population. With the increasing prevalence of CHD and CIS, and especially the rising incidence of CVD in young individuals (24), this tool may help individuals to understand their risk of CHD and CIS. The relative risk score provided by the model could raise awareness of early vascular aging among young individuals, to motivate them to change lifestyles following medical advice. The effectiveness of this model originates from the underlying well-performing models. When testing the performance in the sequential dataset, the AUC of CHD and CIS reached 0.905 and 0.889, respectively. Contrary to previous research (4-6), the good performance of our models may be attributed to the resolution of the imbalanced classification between controls and cases with a combination of the random downsampling and ensemble learning to ensure the maximal usage of the controls. This combination can address the data ambiguity generated from random sampling.

The relationships between CVD diseases and various indicators were also illustrated in this study. These results were consistent with our hypothesis, that the significantly related indicators of CHD and CIS were highly overlapped with each other, and only a few indicators were different. Specifically, age, baPWV, hypertension, and LDL-C were considered risk factors in both models. However, HbA1c, CEA, PLT were only found to contribute to risk in the CHD model, and ABI was only found to be crucial in the CIS model. Both ABI (25) and baPWV, as indicators of vascular stiffness, have been gradually acknowledged and applied in clinical practice. Hyperlipidemia, hyperglycemia, and hypertension are recognized as canonical risk factors for CVD (26). In this perspective, our research demonstrated that hypertension is a common risk factor in CHD and CIS and it may have a more significant effect in males than in females. This phenomenon might be attributed to the gender-specific differences in cell senescence pathways and mitochondrial function. Such differences would lead to different levels of hypertension-induced organ damage in different genders (27). Surprisingly, a negative relationship between LDL-C and disease risk was noted in both models, and also with TC in the CHD model. This may be partly due to the higher proportion of patients taking lipid-lowering drugs (Tables S3,S4). Sachdeva *et al.* also witnessed a negative correlation between LDL-C and CHD risk in the European population, suggesting that it might be caused by the shifts in the prevalence of other cardiovascular risk factors (28). Furthermore, it is well-known that a majority of CHD patients experience chronic low-grade inflammation (29). Consistent with previous studies (30,31), we identified CEA, one of the inflammatory indicators (32), as a potential biomarker of CHD. A total of 7.67% of patients presented with abnormally high CEA values (CEA greater than 0.5 ng/mL), compared to 3.13% of controls with abnormal values (chi-square test P<0.001). Notably, a portion of control individuals without CHD showed similarities in indicators such as age, baPWV, and HbA1c, as CHD patients, but controls had lower inflammatory levels. CVD is a complex disease, but the indicators contained in the traditional model [such as age, smoking status, and systolic blood pressure (SBP)] can only reflect part of the body's condition. As incorporating non-traditional factors can improve the effectiveness of the model (33), adding indicators that reflect the immune system may be beneficial. Unlike SII, CEA is not in the routine set of tests, and the clinical value of this tumor marker warrants further large-scale research.

There were some potential limitations to this study. Calibration analysis showed that our models might overestimate the risk score, that is, the low-risk population might be classified as medium-to-high risk. However, such

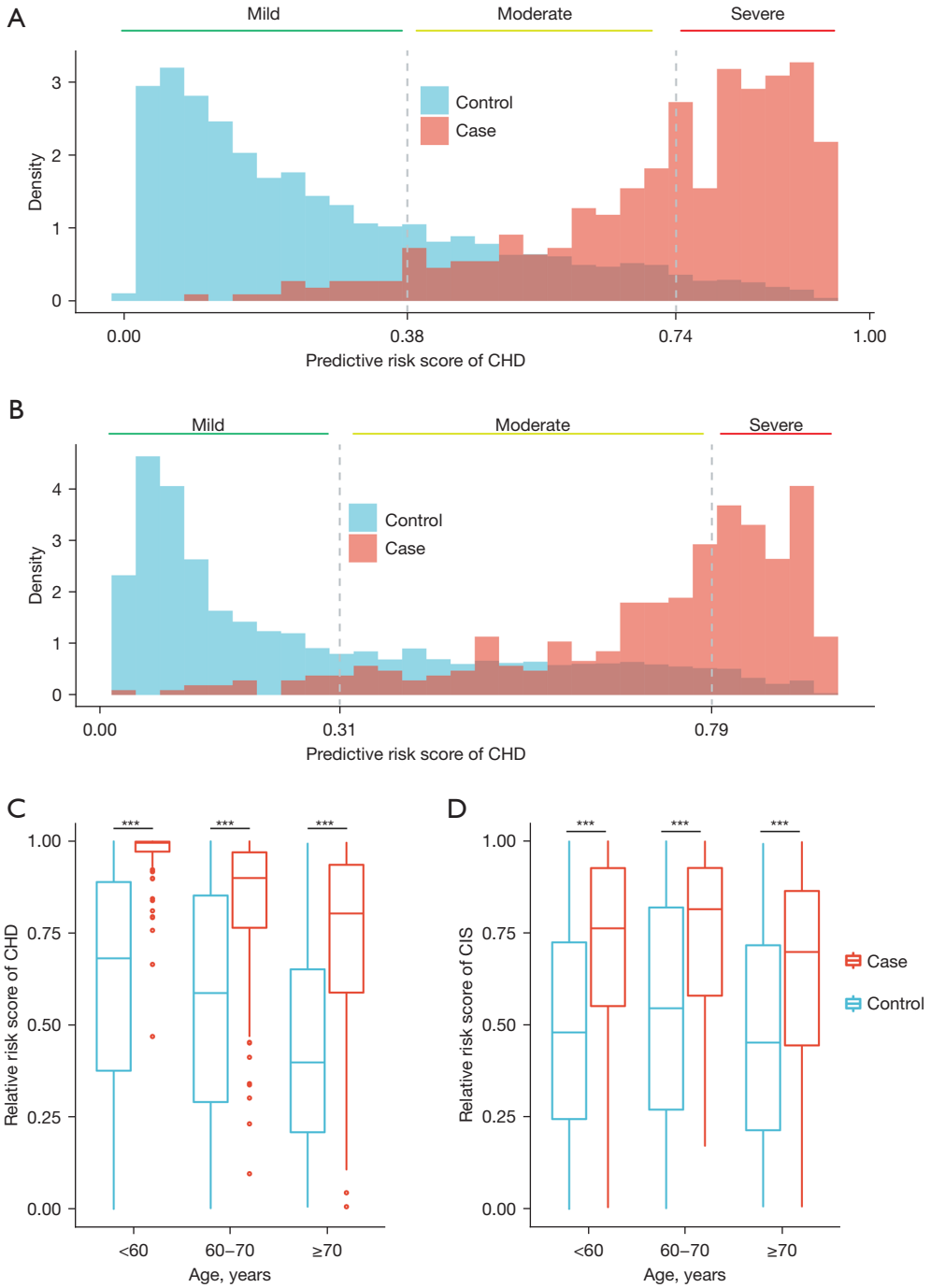

Figure 5 The performance of the risk stratification model in the sequential validation. (A) and (B) represent the distribution of CHD and CIS risk scores. (C) and (D) show the boxplots of the CHD and CIS relative risk scores. Rank-sum test, *** represents significance levels P<0.001. CHD, coronary heart disease; CIS, cerebral ischemic stroke.

overestimation would not affect the relative risk, because the relative risk is based on ranking. In addition, it should be noted that this study only included specific medical records from an Asian population. Previous studies have suggested that the genome and the metagenome of gut microbiota may also affect the risk of CVD (34,35). The inclusion

of this information may provide a better understanding of CVD risk among the population. Therefore, we are currently conducting a 10-year prospective cohort study including genome and metagenome sequencing data of all the participants in China (ChiCTR2100042724).

Conclusions

Herein, we developed 2 well-performing machine learning models for predicting CHD and CIS. The relationships between the clinical indicators and diseases were consistent with previous studies. Based on our models, we constructed a CHD and CIS risk stratification tool for the Asian population.

Acknowledgments

We would like to thank the general physicians, especially those from the Department of Geriatrics of Tongji Hospital, Tongji Medical College, Huazhong University of Science and Technology for their dedication, commitment, and contribution.

Funding: This work was supported by the National Key Research and Development Program of China (No. 2020YFC2008002; principal investigator CZ) and the Major Technology Innovation of Hubei Province (No. 2019ACA141). The funding sources declare that they had no involvement in the process of this study or manuscript preparation. The contents do not reflect the official views of the government of the Hubei province.

Footnote

Reporting Checklist: The authors have completed the TRIPOD reporting checklist. Available at https://atm.amegroups.com/article/view/10.21037/atm-22-1916/rc

Data Sharing Statement: Available at https://atm.amegroups.com/article/view/10.21037/atm-22-1916/dss

Peer Review File: Available at https://atm.amegroups.com/article/view/10.21037/atm-22-1916/prf

Conflicts of Interest: All authors have completed the ICMJE uniform disclosure form (available at https://atm.amegroups.com/article/view/10.21037/atm-22-1916/coif). All authors declare that this study was supported by the National Key Research and Development Program of China (No. 2020YFC2008002; principal investigator CZ) and the Major Technology Innovation of Hubei Province (No. 2019ACA141). BC, LY, YL, XJ, YB, and TL are employees of BGI-Shenzhen. The authors have no other conflicts of interest to declare.

Ethical Statement: The authors are accountable for all aspects of the work in ensuring that questions related to the accuracy or integrity of any part of the work are appropriately investigated and resolved. The study was conducted in accordance with the Declaration of Helsinki (as revised in 2013). The study was approved by the Medical Ethics Committee at Tongji Medical College, Huazhong University of Science and Technology (No. TJ-IRB20191215) and individual consent for this retrospective analysis was waived.

References

1. Liu S, Li Y, Zeng X, et al. Burden of Cardiovascular Diseases in China, 1990-2016: Findings From the 2016 Global Burden of Disease Study. JAMA Cardiol 2019;4:342-52.
2. The Writing Committee of the Report on Cardiovascular Health and Diseases in China. Report on Cardiovascular Health and Diseases in China 2019: an Updated Summary. Chinese Circulation Journal 2020;35:833-54.
3. Ngiam KY, Khor IW. Big data and machine learning algorithms for health-care delivery. Lancet Oncol 2019;20:e262-73.
4. Tama BA, Im S, Lee S. Improving an Intelligent Detection System for Coronary Heart Disease Using a Two-Tier Classifier Ensemble. Biomed Res Int 2020;2020:9816142.
5. Dinh A, Miertschin S, Young A, et al. A data-driven approach to predicting diabetes and cardiovascular disease with machine learning. BMC Med Inform Decis Mak 2019;19:211.
6. Wu Y, Fang Y. Stroke Prediction with Machine Learning

Methods among Older Chinese. Int J Environ Res Public Health 2020;17:1828.
7. Gooding HC, de Ferranti SD. Cardiovascular risk assessment and cholesterol management in adolescents: getting to the heart of the matter. Curr Opin Pediatr 2010;22:398-404.
8. Nivette A, Ribeaud D, Murray A, et al. Non-compliance with COVID-19-related public health measures among young adults in Switzerland: Insights from a longitudinal cohort study. Soc Sci Med 2021;268:113370.
9. Liu J, Hong Y, D'Agostino RB Sr, et al. Predictive value for the Chinese population of the Framingham CHD risk assessment tool compared with the Chinese Multi-Provincial Cohort Study. JAMA 2004;291:2591-9.
10. Loscalzo J. Harrison's Cardiovascular Medicine, 3rd Edition. 2017.
11. Stekhoven DJ, Bühlmann P. MissForest--non-parametric missing value imputation for mixed-type data. Bioinformatics 2012;28:112-8.
12. Thompson HW, Mera R, Prasad C. The Analysis of Variance (ANOVA). Nutr Neurosci 1999;2:43-55.
13. Guyon I, Weston J, Barnhill S, et al. Gene Selection for Cancer Classification Using Support Vector Machines. Mach Learn 2002;46:389-422.
14. Kursa M, Rudnicki W. Feature Selection with Boruta Package. J Stat Softw 2010;36:1-13.
15. Breiman L. Random Forests. Mach Learn 2001;45:5-32.
16. Pedregosa F, Varoquaux G, Gramfort A, et al. Scikit-learn: Machine Learning in Python. J Mach Learn Res 2012;12:2825-30.
17. Lemaître G, Nogueira F, Aridas C. Imbalanced-learn: A Python Toolbox to Tackle the Curse of Imbalanced Datasets in Machine Learning. J Mach Learn Res 2017;18:1-5.
18. Lundberg S, Lee SI. A Unified Approach to Interpreting Model Predictions. NIPS'17: Proceedings of the 31st International Conference on Neural Information Processing Systems 2017;4768-77.
19. Wilson PW, D'Agostino RB, Levy D, et al. Prediction of coronary heart disease using risk factor categories. Circulation 1998;97:1837-47.
20. Dufouil C, Beiser A, McLure LA, et al. Revised Framingham Stroke Risk Profile to Reflect Temporal Trends. Circulation 2017;135:1145-59.
21. Rooke TW, Hirsch AT, Misra S, et al. 2011 ACCF/AHA focused update of the guideline for the management of patients with peripheral artery disease (updating the 2005 guideline): a report of the American College of Cardiology Foundation/American Heart Association Task Force on Practice Guidelines: developed in collaboration with the Society for Cardiovascular Angiography and Interventions, Society of Interventional Radiology, Society for Vascular Medicine, and Society for Vascular Surgery. Catheter Cardiovasc Interv 2012;79:501-31.
22. Takashima N, Turin TC, Matsui K, et al. The relationship of brachial-ankle pulse wave velocity to future cardiovascular disease events in the general Japanese population: the Takashima Study. J Hum Hypertens 2014;28:323-7.
23. Regitz-Zagrosek V, Kararigas G. Mechanistic Pathways of Sex Differences in Cardiovascular Disease. Physiol Rev 2017;97:1-37.
24. Andersson C, Vasan RS. Epidemiology of cardiovascular disease in young individuals. Nat Rev Cardiol 2018;15:230-40.
25. Perlstein TS, Creager MA. The ankle-brachial index as a biomarker of cardiovascular risk: it's not just about the legs. Circulation 2009;120:2033-5.
26. Mahmood SS, Levy D, Vasan RS, et al. The Framingham Heart Study and the epidemiology of cardiovascular disease: a historical perspective. Lancet 2014;383:999-1008.
27. Colafella KMM, Denton KM. Sex-specific differences in hypertension and associated cardiovascular disease. Nat Rev Nephrol 2018;14:185-201.
28. Sachdeva A, Cannon CP, Deedwania PC, et al. Lipid levels in patients hospitalized with coronary artery disease: an analysis of 136,905 hospitalizations in Get With The Guidelines. Am Heart J 2009;157:111-117.e2.
29. Golia E, Limongelli G, Natale F, et al. Inflammation and cardiovascular disease: from pathogenesis to therapeutic target. Curr Atheroscler Rep 2014;16:435.
30. Ishizaka N, Ishizaka Y, Toda E, et al. Are serum carcinoembryonic antigen levels associated with carotid atherosclerosis in Japanese men? Arterioscler Thromb Vasc Biol 2008;28:160-5.
31. Bae U, Shim JY, Lee HR, et al. Serum carcinoembryonic antigen level is associated with arterial stiffness in healthy Korean adult. Clin Chim Acta 2013;415:286-9.
32. Gold P, Freedman SO. Specific carcinoembryonic antigens of the human digestive system. J Exp Med 1965;122:467-81.
33. Lin JS, Evans CV, Johnson E, et al. Nontraditional Risk Factors in Cardiovascular Disease Risk Assessment: Updated Evidence Report and Systematic Review

for the US Preventive Services Task Force. JAMA 2018;320:281-97.
34. Wang Y, Wang JG. Genome-Wide Association Studies of Hypertension and Several Other Cardiovascular Diseases. Pulse (Basel) 2019;6:169-86.
35. Witkowski M, Weeks TL, Hazen SL. Gut Microbiota and Cardiovascular Disease. Circ Res 2020;127:553-70.

(English Language Editors: J. Teoh and J. Jones)

Cite this article as: Chen B, Ruan L, Yang L, Zhang Y, Lu Y, Sang Y, Jin X, Bai Y, Zhang C, Li T. Machine learning improves risk stratification of coronary heart disease and stroke. Ann Transl Med 2022;10(21):1156. doi: 10.21037/atm-22-1916

Appendix 1

Supplemental Methods

Measurement of clinical variables

Lifestyle variables

Lifestyle variables included age, body mass index (BMI), drinking, and smoking. BMI was calculated as weight in kilograms divided by the square of height in meters. Drinking status was divided into the following 2 categories: (I) non-drinkers (participants who never drink or who drink less than once a month, and the alcohol content is less than 10%); and (II) drinkers (patients who drink once or more a month, or the alcohol content is more than 10%). Smoking status was divided into the following 2 groups: (I) non-smokers (patients who have never smoked before); and (II) current smokers (patients who still smoke) or past smokers (those who used to smoke but have now quit).

Medical history

Histories of hyperlipidemia, hypertension, and diabetes mellitus were obtained from in-person interviews. The diagnosis of hyperlipidemia was based on any one of the following: (I) low-density lipoprotein cholesterol (LDL-C) ≥4.14 mmol/L; (II) total cholesterol (TC) >6.45 mmol/L; and (III) triglyceride ≥2.26 mmol/L. The diagnosis of hypertension was based on resting blood pressure. If the resting blood pressure was >140/90 mmHg, the individual was diagnosed with hypertension. The diagnosis of diabetes mellitus was based any one of the following: (I) fasting plasma glucose ≥7.0 mmol/L; (II) plasma glucose ≥11.1 mmol/L 2 hours after the consumption of a drink containing 75 g of glucose; (III) symptoms of high blood sugar and a casual plasma glucose ≥11.1 mmol/L; and (IV) hemoglobin A1c ≥48 mmol/mol.

Physical examination

Blood pressure, brachial-ankle pulse wave velocity (baPWV), and ankle-brachial index (ABI) were measured using the Vascular Profiler BP-203RPEIII (Omron, Kyoto, Japan). The examination room was maintained at 26 ℃. Trained technicians placed 4 pressure cuffs on the participants (one on the upper part of each arm and one on each ankle). Participants were then examined after 10 minutes of rest in the supine position. The device simultaneously recorded bilateral systolic and diastolic blood pressure, ABI, and baPWV, the latter of which was calculated as the ratio of traveled distance (which was automatically estimated from body height) divided by the transit time of the pulse wave between the brachial and posterior tibial arteries. The average of 2-sided baPWV values and 2-sided ABI values were recorded for analysis.

Blood examination

Blood examination (routine blood tests and blood biochemical index tests) were measured using fasting venous blood samples. Routine blood tests were performed using the XN9000 system (Sysmex, Kobe, Japan). Blood biochemical indices, including liver function, renal function, blood lipid profile, fasting blood glucose, HbA1c, and uric acid, were measured using the COBAS 8000 c701 system (Roche, Basel, Switzerland).

Urine examination

Urinary elements were measured using the UF-1000i fully automatic urine analyzer (Sysmex, Kobe, Japan). Urinary chemistry elements were measured using the Siemens Atlas Urine Chemistry Analyzer (Siemens, Erlangen, Germany). The estimated glomerular filtration rate was calculated according to the Cockcroft-Gault formula.

Framingham risk score

The probabilities of CHD and CIS for 10 years are calculated using the following formula:

https://dx.doi.org/10.21037/atm-22-1916

$$P = 1 - Sb(10) \exp(L\text{-}M) \quad [1]$$

where Sb is the probability of survival free for 10 years, L is the linear combination of an individual's risk factor values and the corresponding coefficients, and M is simply L evaluated at the mean of all the covariates.

For female probability of CHD, M = 9.92545, S(10) = 0.96246, and L are calculated as follows:

L = 0.33766 × Age – 0.00268 × Age2 – 0.26138 (if cholesterol < 160) + 0.20771 (if 200 ≤ cholesterol < 240) + 0.24385 (if 240 ≤ cholesterol < 280) + 0.53513 (if cholesterol ≥ 280) + 0.84312 (if HDL-C <35) + 0.37796 (if 35 ≤ HDL-C < 45) + 0.19785 (if 45 ≤ HDL-C < 50) - 0.42951 (if HDL-C ≥ 60) - 0.53363 (systolic blood pressure [SBP] < 120 and DBP <80) - 0.06773 (130 ≤ SBP < 140 or 85 ≤ diastolic blood pressure [DBP] <90) + 0.26288 (140 ≤ SBP < 160 or 90 ≤ DBP <100) + 0.46573 (SBP ≥ 160 or DBP ≥ 100) + 0.59626 (if diabetic) + 0.29246 (if smoker) [2]

For male probability of CHD, M = 3.0975, S (10) = 0.90015, and L were calculated as follows:

L = 0.04826 × Age – 0.65945 (if cholesterol < 160) + 0.17692 (if 200 ≤ cholesterol < 240) + 0.50539 (if 240 ≤ cholesterol < 280) + 0.65713 (if cholesterol ≥ 280) + 0.49744 (if HDL-C < 35) + 0.24310 (if 35 ≤ HDL-C < 45) - 0.05107 (if 50 ≤ HDL-C < 60) - 0.48660 (if HDL-C ≥ 60) -0.00226 (SBP < 120 and DBP <80) + 0.28320 (130 ≤ SBP < 140 or 85 ≤ DBP <90) + 0.52168 (140 ≤ SBP < 160 or 90 ≤ DBP <100) + 0.61859 (SBP ≥ 160 or DBP ≥ 100) + 0.42839 (if diabetic) + 0.52337 (if smoker) [3]

For female probability of CIS, M = 6.6170719, S (10) = 0.95911, and L were calculated as follows:

L = 0.87938 × (Age/10) + 0.51127 (if smoker) – 0.03035 (if CVD) + 1.20720 (if atrial fibrillation) + 0.39796 (if Age ≥ 65) + 1.07111 (if Age < 65 and diabetic) + 0.06565 (if age ≥ 65 and diabetic) + 0.13085 (if taking antihypertensive drugs) + 0.17234 × (SBP-120)/10 (if taking antihypertensive drugs) + 0.11303 × (SBP-120)/10 (if not taking antihypertensive drugs) [4]

For male probability of CIS, M = 4.4227101, S (10) = 0.94451, and L were calculated as follows:

L = 0.49716 × (Age/10) + 0.47254 (if smoker) + 0.45341 (if CVD) + 0.08064 (if atrial fibrillation) + 0.45426 (if age ≥ 65) + 1.35304 (if age < 65 and diabetic) + 0.34385 (if age ≥ 65 and diabetic) + 0.82598 (if taking antihypertensive drugs) + 0.09793 × (SBP-120)/10 (if taking antihypertensive drugs) + 0.27323 × (SBP-120)/10 (if not taking antihypertensive drugs) [5]

https://dx.doi.org/10.21037/atm-22-1916

Table S1 The characteristics of the study population

Variables	Population (N=8,624)
Basic characteristics	
Age, year	51.9±11.4
Sex	
Male	6,152 (71.3)
Female	2,472 (28.7)
Smoker	2,777 (32.2)
Drinker	3,823 (44.3)
BMI, kg/m^2	24.6±3.1
Medical histories	
Atrial fibrillation	19 (0.2)
Chronic obstructive pulmonary disease	11 (0.1)
Coronary heart disease	339 (3.9)
Diabetes	538 (6.2)
Epilepsy	0 (0)
Hemorrhagic stroke	11 (0.1)
Hyperlipidemia	464 (5.4)
Hypertension	1,928 (22.4)
Hypoglycemia	0 (0)
Hypotension	1 (0.01)
Ischemic stroke	339 (3.9)
Myocardiopathy	2 (0.02)
Sick sinus syndrome	2 (0.02)
Transient ischemic attack	1 (0.01)
Valvular heart disease	2 (0.02)
Vascular stiffness	2,427 (28.1)
Medication histories	
Alpha-glucosidase inhibitor	137 (1.6)
Angiotensin converting enzyme inhibitor	144 (1.7)
Angiotensin receptor blocker	652 (7.6)
Antiadrenergic	346 (4)
Antiarrhythmia	6 (0.07)
Anticoagulant	6 (0.07)
Antidiabetic drug	153 (1.8)
Antihypertensive drug	1,431 (16.6)
Antiplatelet	373 (4.3)
Biguanide	143 (1.7)
Calcium channel blocker	820 (9.5)
Dipeptidyl peptidase-4 inhibitor	28 (0.3)
Diuretic	126 (1.5)
Glinide	44 (0.5)
Glucagon-like peptide-1 receptor agonist	0 (0)
Hyperthyroidism	16 (0.2)
Hypothyroidism	110 (1.3)
Insulin	84 (1)
Lipid lowering drug	434 (5)
Nitrates	15 (0.2)
Others antidiabetic drug	77 (0.9)
Others antihypertensive drug	313 (3.6)
Sulfonylurea	74 (0.9)
Thiazolidinedione	20 (0.2)
Uric acid lowering drug	59 (0.7)
Clinical measurements	
Ankle brachial index	1.1±0.07
Brachial-ankle pulse wave velocity, cm/s	1,409.7±256.5
Diastolic blood pressure, mmHg	81.7±11.4
Systolic blood pressure, mmHg	126.3±16.9
Heart rate, time/min	74.5±10.2
Heart rhythm	31 (0.4)
Blood test	
Absolute basophil count, 10^9/L	0.03±0.02
Absolute eosinophil count, 10^9/L	0.2±0.1
Absolute lymphocyte count, 10^9/L	1.9±0.6
Absolute monocyte count, 10^9/L	0.4±0.1
Absolute neutrophil count, 10^9/L	3.3±1.1
Albumin, g/L	44.9±2.6
Alkaline phosphatase, U/L	64±24.9
Alpha-fetoprotein, ng/ml	3.6±1.9
Mean corpuscular hemoglobin concentration, g/L	339.4±12.1
Mean hemoglobin content, pg	30.7±2
Mean RBC volume, fL	90.5±5
Carcinoembryonic antigen, ng/mL	2.1±3.8
Creatinine, μmol/L	75.8±20.6
Direct bilirubin, μmol/L	3.5±1.8
Erythrocyte sedimentation rate, nm/H	5.3±5.8
Estimated glomerular filtration rate, mL/min/1.73 m^2	71.2±19.5
Fasting blood glucose, mmol/L	5.2±1.2
Gamma glutamyl transpeptidase, U/L	37.6±50.2
Globulin, g/L	29.4±3.3
Glutamate-pyruvate transaminase, U/L	23.5±26.2
Glutamic oxaloacetic transaminase, U/L	21.9±13.4
Hematocrit, %	43.5±4
Hemoglobin, g/L	147.6±14.7
Hemoglobin A1C, %	5.8±0.7
High-density lipoprotein cholesterol, mmol/L	1.2±0.3
Low density lipoprotein cholesterol, mmol/L	2.9±0.8
Mean platelet volume, fL	10.1±1.7
Percentage of basophil, %	0.5±0.3
Percentage of eosinophils, %	2.6±2
Percentage of lymphocyte, %	33.8±7.4
Percentage of monocyte, %	7±1.8
Percentage of neutrophils, %	56.2±7.9
Platelet count, 10^9/L	216.6±54.1
Platelet large cell ratio, %	32.3±6.9
Platelet crit, %	0.2±0.06
Platelet distribution width, fL	14.2±2.3
Prostate-specific antigen, ng/mL	1.2±2.1
Red blood cell, 10^{12}/L	4.8±0.5
Total bilirubin, μmol/L	13.0±5.1
Total cholesterol, mmol/L	4.7±0.9
Total protein, g/L	74.4±4.1
Triglyceride, mmol/L	1.6±1.4
Urea, mmol/L	5.2±1.3
Uric acid, mmol/L	352.7±90.1
White blood cell count, 10^9/L	5.9±1.6
Urine test	
Fungi	9 (0.1)
Ketone	111 (1.3)
Nitrite	67 (0.8)
Pathological cast count, /mL	0.1±0.2
Small round epithelial cell	177 (2.1)
Urinary cast count, /mL	0.3±0.4
Urinary erythrocyte morphology	479 (5.6)
Urinary occult blood	1,106 (12.8)
Urine bilirubin	293 (3.4)
Urine crystal	676 (7.8)
Urine epithelial cells count, /mL	8.6±18.6
Urine glucose	90 (1)
Urine pH	6.2±0.7
Urine protein	351 (4.1)
Urine red blood cell count, /mL	20.9±374.9
Urine specific gravity	1±0.007
Urine white blood cell	597 (6.9)
Urine white blood cell count, /mL	21.8±179
Urobilinogen	8 (0.09)

Continuous variables were described as mean ± SD. Categorical variables are described as number (percentage). BMI, body mass index; RBC, red blood cell; SD, standard deviation.

https://dx.doi.org/10.21037/atm-22-1916

Table S2 Characteristics of the CHD dataset (N=7,698)

Variables	Training (N=5,136)	Random testing (N=1,284)	Sequential testing (N=1,278)
Basic characteristics			
Age	52.8±9.8	52.5±10.1	53.2±10.5
Male	3,721 (72.4)	900 (70.1)	927 (72.5)
Smoker	1,686 (32.8)	395 (30.8)	466 (36.5)
Drinker	2,245 (43.7)	538 (41.9)	670 (52.4)
BMI, kg/m^2	24.7±3.03	24.6±2.98	24.6±3.1
Cardiovascular medical history			
CHD	219 (4.3)	57 (4.4)	63 (4.9)
CIS	25 (0.5)	5 (0.4)	7 (0.5)
Clinical measurements			
SBP, mmHg	126.7±16.6	126.5±16.7	126.7±17.8
DBP, mmHg	82.4±11.5	81.9±11.3	81±11.4
LDL-C, mmol/L	2.9±0.8	2.9±0.8	2.8±0.8
HDL-C, mmol/L	1.2±0.3	1.2±0.3	1.2±0.3
TC, mmol/L	4.8±0.9	4.8±0.9	4.5±0.9
TG, mmol/L	1.7±1.4	1.7±1.5	1.7±1.6
FBG, mmol/L	5.3±1.2	5.3±1.2	5.2±1.2
HbA1c, %	5.8±0.7	5.8±0.7	5.7±0.7
baPWV, cm/s	1,416.6±247.5	1,411.2±241.1	1,430.7±270.7
<1,400	2,807 (54.7)	711 (55.4)	664 (52)
1,400–1,800	1,984 (38.6)	476 (37.1)	507 (39.7)
≥1,800	345 (6.7)	97 (7.6)	107 (8.4)
ABI	1.1±0.07	1.1±0.07	1.1±0.07
<0.9	28 (0.5)	15 (1.2)	7 (0.5)
0.9–1.4	5,100 (99.3)	1,267 (98.7)	1,270 (99.4)
≥1.4	8 (0.2)	2 (0.2)	1 (0.1)

Continuous variables are described as mean ± SD. Categorical variables are described as number (percentage). CHD, coronary heart disease; BMI, body mass index; CIS, cerebral ischemic stroke; SBP, systolic blood pressure; DBP, diastolic blood pressure; HDL-C, high-density lipoprotein cholesterol; LDL-C, low-density lipoprotein cholesterol; TC, total cholesterol; TG, triglyceride; FBG, fasting blood glucose; HbA1c, hemoglobin A1C; baPWV, brachial-ankle pulse wave velocity; ABI, ankle brachial index; SD, standard deviation.

https://dx.doi.org/10.21037/atm-22-1916

Table S3 Characteristics of the CIS dataset (N=8,322)

Variables	Training (N=5,503)	Random testing (N=1,375)	Sequential testing (N=1,444)
Basic characteristics			
Age	51.5±10.9	51.6±11.2	50.7±12.1
Male	3,899 (70.9)	961 (69.9)	1,027 (71.1)
Smoker	1,752 (31.8)	418 (30.4)	491 (34)
Drinker	2,416 (43.9)	571 (41.5)	740 (51.2)
BMI, kg/m^2	24.6±3.1	24.5±3.1	24.4±3.2
Cardiovascular medical history			
CHD	26 (0.5)	4 (0.3)	7 (0.5)
CIS	230 (4.2)	52 (3.8)	57 (3.9)
Clinical measurements			
SBP, mmHg	126.2±16.5	126.2±17.2	125.6±17.6
DBP, mmHg	82±11.4	82±11.6	80.4±11.3
LDL-C, mmol/L	2.9±0.8	2.9±0.7	2.8±0.8
HDL-C, mmol/L	1.2±0.3	1.2±0.3	1.2±0.3
TC, mmol/L	4.8±0.9	4.7±0.9	4.5±0.9
TG, mmol/L	1.6±1.4	1.7±1.5	1.6±1.5
FBG, mmol/L	5.2±1.2	5.2±1.2	5.1±1.1
HbA1c, %	5.8±0.7	5.8±0.7	5.7±0.7
baPWV, cm/s	1401.8±247.7	1408.7±252.7	1400.7±272.8
<1,400	3,124 (56.8)	780 (56.7)	823 (57)
1,400–1,800	2,017 (36.7)	494 (35.9)	514 (35.6)
>1,800	362 (6.6)	101 (7.3)	107 (7.4)
ABI	1.1±0.07	1.1±0.06	1.1±0.07
<0.9	42 (0.8)	6 (0.4)	7 (0.5)
0.9–1.4	5,453 (99.1)	1,368 (99.5)	1,436 (99.4)
>1.4	8 (0.1)	1 (0.1)	1 (0.1)

Continuous variables are described as mean ± SD. Categorical variables are described as number (percentage). CIS, cerebral ischemic stroke; BMI, body mass index; CHD, coronary heart disease; SBP, systolic blood pressure; DBP, diastolic blood pressure; LDL-C, low-density lipoprotein cholesterol; HDL-C, high-density lipoprotein cholesterol; TC, total cholesterol; TG, triglyceride; FBG, fasting blood glucose; HbA1c, hemoglobin A1C; baPWV, brachial-ankle pulse wave velocity; ABI, ankle brachial index; SD, standard deviation.

https://dx.doi.org/10.21037/atm-22-1916

Table S4 Selected features by ANOVA, RFE, and Boruta

Disease	Overlap features	Unique features
CHD	TC, baPWV, AMC, RBC count, LDL-C, PSA, creatinine, monocyte, SBP, MCV, CEA, eGFR, platelet count, FBG, age, urea	UA, HDL-C, lymphocyte, HbA1c, TG, heart rate, BMI
Ischemic stroke		MCH, WBC count, ABI, ANC, ALP, globulin

Features were collected into category "overlap features" if they presented both in CHD and ischemic. Otherwise, features will be collected into "unique features". ANOVA, analysis of variance; RFE, recursive feature elimination; CHD, coronary heart disease; TC, total cholesterol; baPWV, brachial-ankle pulse wave velocity; AMC, absolute monocyte count; RBC, red blood cell; LDL-C, low-density lipoprotein cholesterol; PSA, prostate specific antigen; SBP, systolic blood pressure; MCV, average red blood cell volume; CEA, carcinoembryonic antigen; eGFR, estimated glomerular filtration rate; FBG, fasting blood glucose; UA, uric acid; HDL-C, high-density lipoprotein cholesterol; HbA1c, hemoglobin A1C; TG, triglyceride; BMI, body mass index; MCH, average hemoglobin content; WBC, white blood cell; ABI, ankle brachial index; ANC, absolute neutrophil count; ALP, alkaline phosphatase.

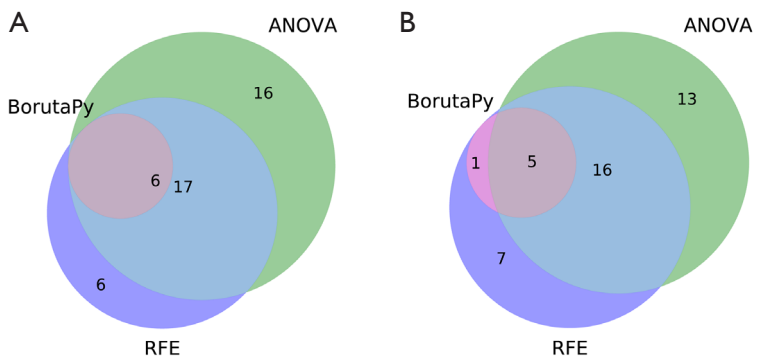

Figure S1 The results of three feature selection methods. (A) Coronary heart disease dataset. (B) Ischemic stroke dataset. ANOVA, analysis of variance; RFE, recursive feature elimination; BorutaPy, boruta for Python.

https://dx.doi.org/10.21037/atm-22-1916

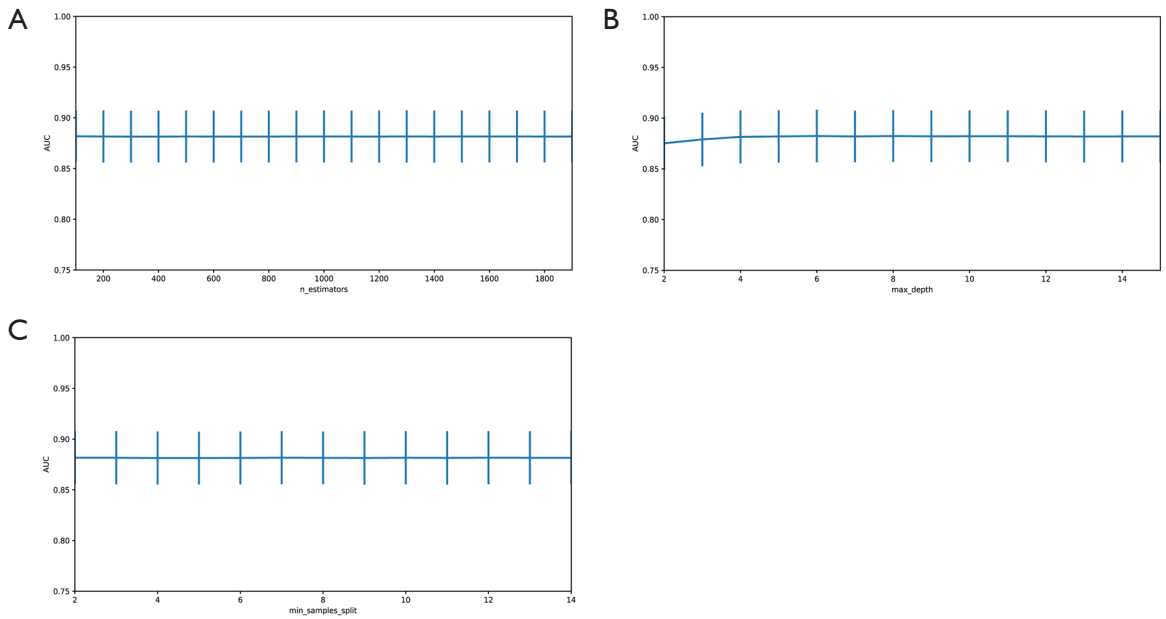

Figure S2 GridSearchCV analysis results of coronary heart disease classification. (A) Model performance with different estimators. (B) Model performance with different maximum depths. (C) Model performance with different minimum sample split. AUC, area under the receiver operating characteristic curve.

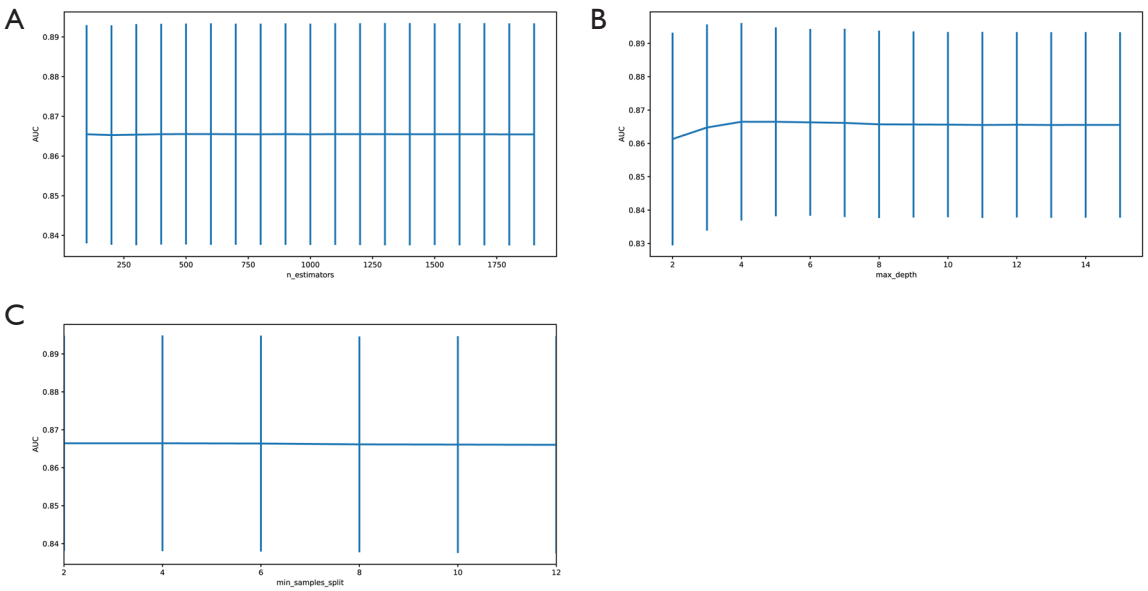

Figure S3 GridSearchCV analysis results of ischemic stroke classification. (A) Model performance with different estimators. (B) Model performance with different maximum depths. (C) Model performance with different minimum sample split. AUC, area under the receiver operating characteristic curve.

https://dx.doi.org/10.21037/atm-22-1916

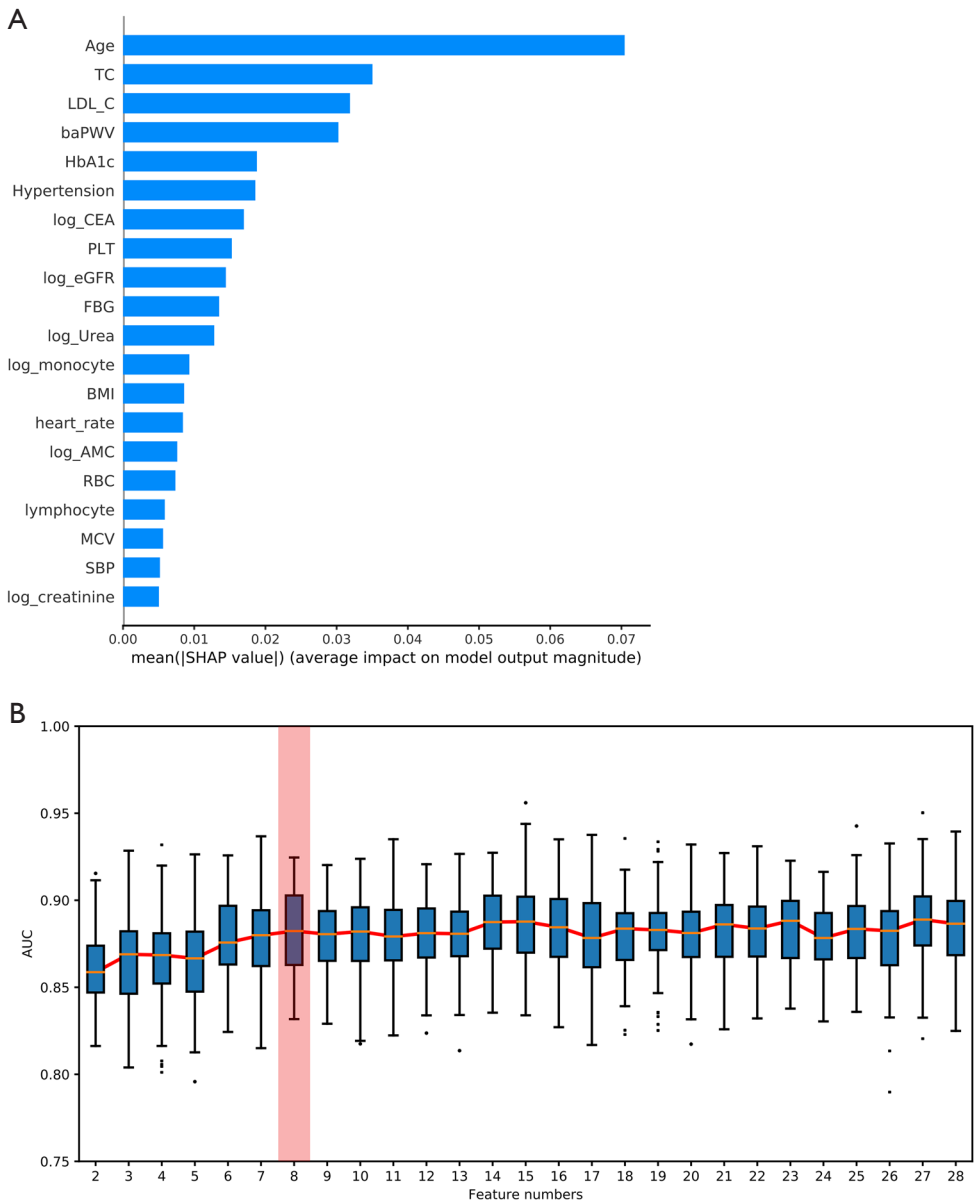

Figure S4 Optimization of the CHD model. (A) Mean absolute SHAP values of each feature in the CHD model during the optimization process. (B) The minimum features required in the CHD model. The inflection point is marked by the red shadow. TC, total cholesterol; LDL-C, low-density lipoprotein cholesterol; baPWV, brachial-ankle pulse wave velocity; HbA1c, hemoglobin A1C; CEA, carcinoembryonic antigen; PLT, platelet; eGFR, estimated glomerular filtration rate; FBG, fasting blood glucose; BMI, body mass index; AMC, absolute monocyte count; RBC, red blood cell; MCV, average red blood cell volume; SBP, systolic blood pressure; SHAP, shapley additive explanations; AUC, area under the receiver operating characteristic curve; CHD, coronary heart disease.

https://dx.doi.org/10.21037/atm-22-1916

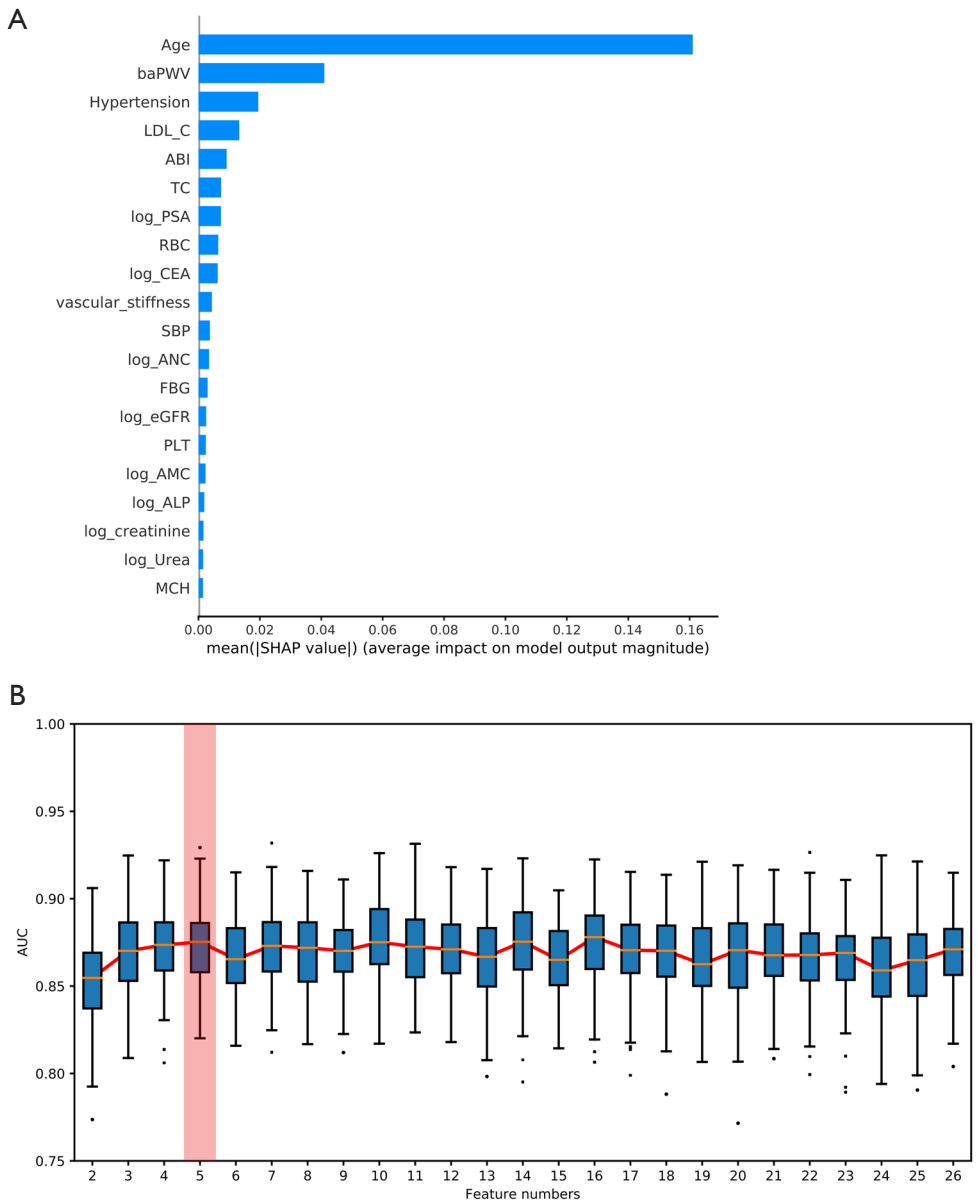

Figure S5 Optimization of the CIS model. (A) Mean absolute SHAP values of each feature in the CIS model during the optimization process. (B) The minimum features required in the CIS model. The inflection point is marked by the red shadow. baPWV, brachial-ankle pulse wave velocity; LDL-C, low-density lipoprotein cholesterol; ABI, ankle brachial index; TC, total cholesterol; PSA, prostate specific antigen; RBC, red blood cell; CEA, carcinoembryonic antigen; SBP, systolic blood pressure; ANC, absolute neutrophil count; FBG, fasting blood glucose; eGFR, estimated glomerular filtration rate; PLT, platelet; AMC, absolute monocyte count; ALP, alkaline phosphatase; MCH, average hemoglobin content; SHAP, shapley additive explanations; AUC, area under the receiver operating characteristic curve; CIS, cerebral ischemic stroke.

https://dx.doi.org/10.21037/atm-22-1916

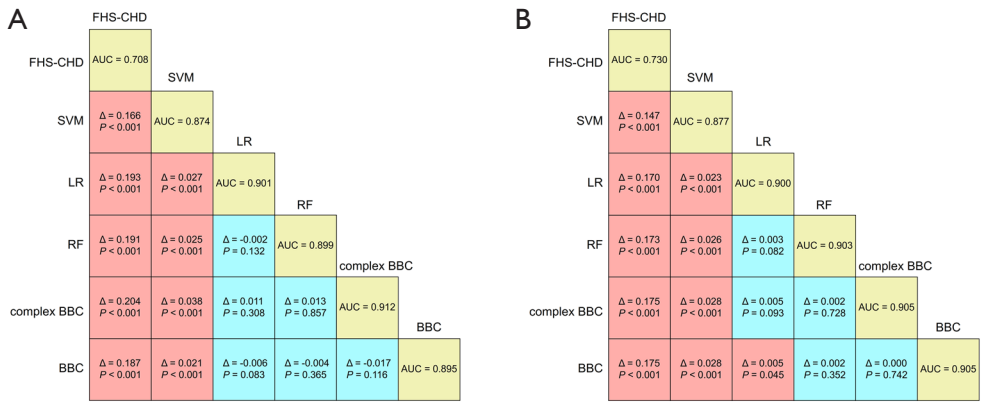

Figure S6 Statistical analysis of the AUCs of the CHD models. (A) Performance of the models using random test data. (B) Performance of the models using sequential test data. Δ represents the difference in AUCs; P represents the result of the ROC curve difference test; the yellow squares represent the AUC values; the square would be red if P < 0.05, and the square would be blue if P≥0.05. FHS-CHD, Framingham risk score of coronary heart disease; SVM, support vector machine; LR, logistic regression; RF, random forest; BBC, balanced bagging classifier; AUC, the area under the receiver operating characteristic curve; CHD, coronary heart disease.

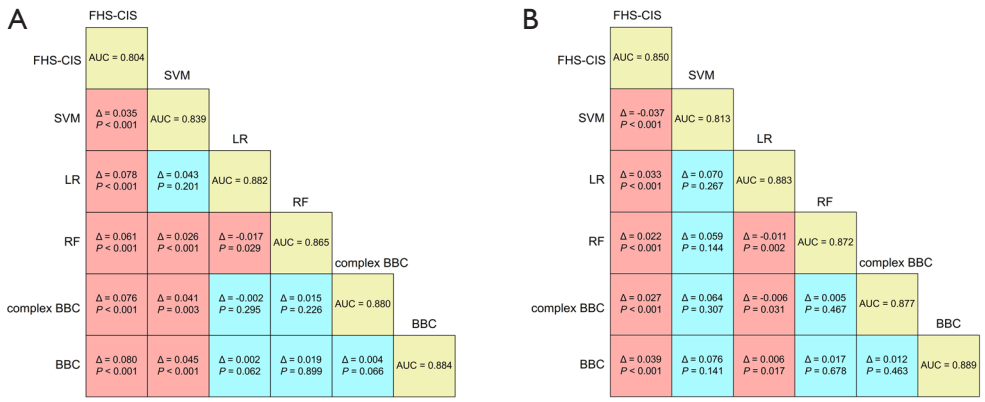

Figure S7 Statistical analysis of the AUCs of the CIS models. (A) Performance of the models using random test data. (B) Performance of the models using sequential test data. Δ represents the difference in AUCs; P represents the result of the ROC curve difference test; the yellow squares represent the AUC values; the square would be red if P < 0.05, and the square would be blue if P≥0.05. FHS-CIS, Framingham risk score of cerebral ischemic stroke; SVM, support vector machine; LR, logistic regression; RF, random forest; BBC, balanced bagging classifier; AUC, the area under the receiver operating characteristic curve; CIS, cerebral ischemic stroke.

https://dx.doi.org/10.21037/atm-22-1916

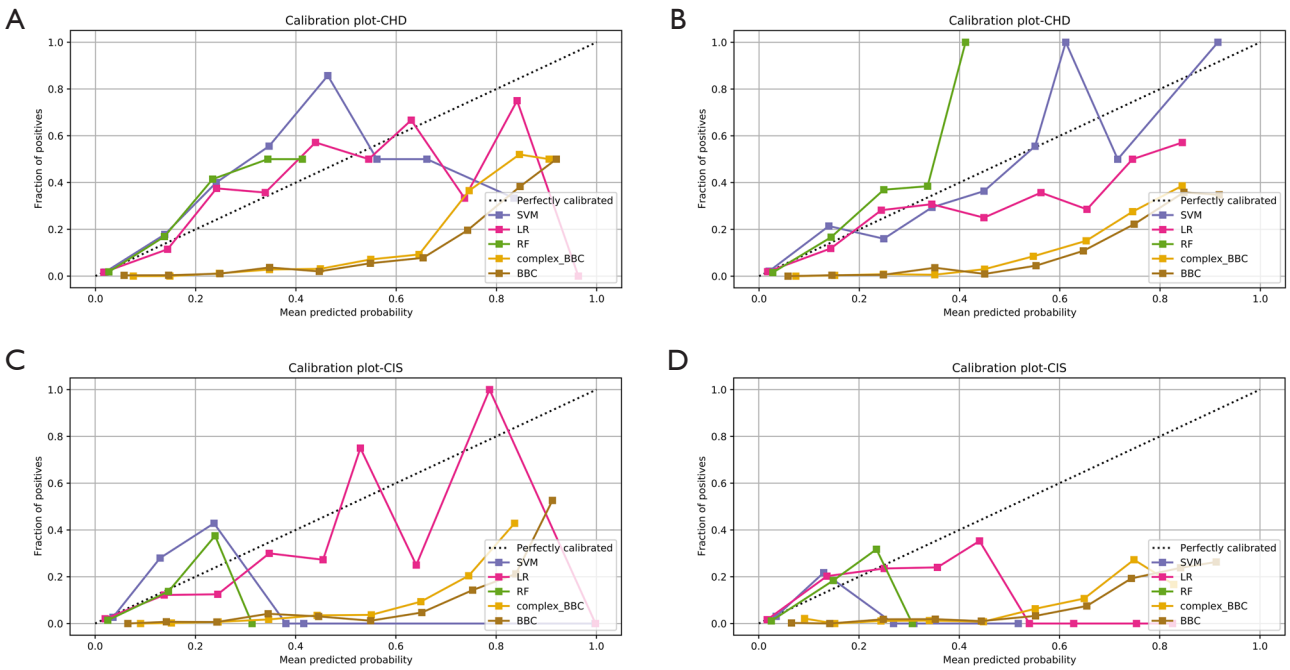

Figure S8 Calibration of each model using different datasets. (A) Random test data of CHD. (B) Sequential test data of CHD. (C) Random test data of CIS. (D) Sequential test data of CIS. CHD, coronary heart disease; SVM, support vector machine; LR, logistic regression; RF, random forest; BBC, balanced bagging classifier; CIS, cerebral ischemic stroke.

https://dx.doi.org/10.21037/atm-22-1916

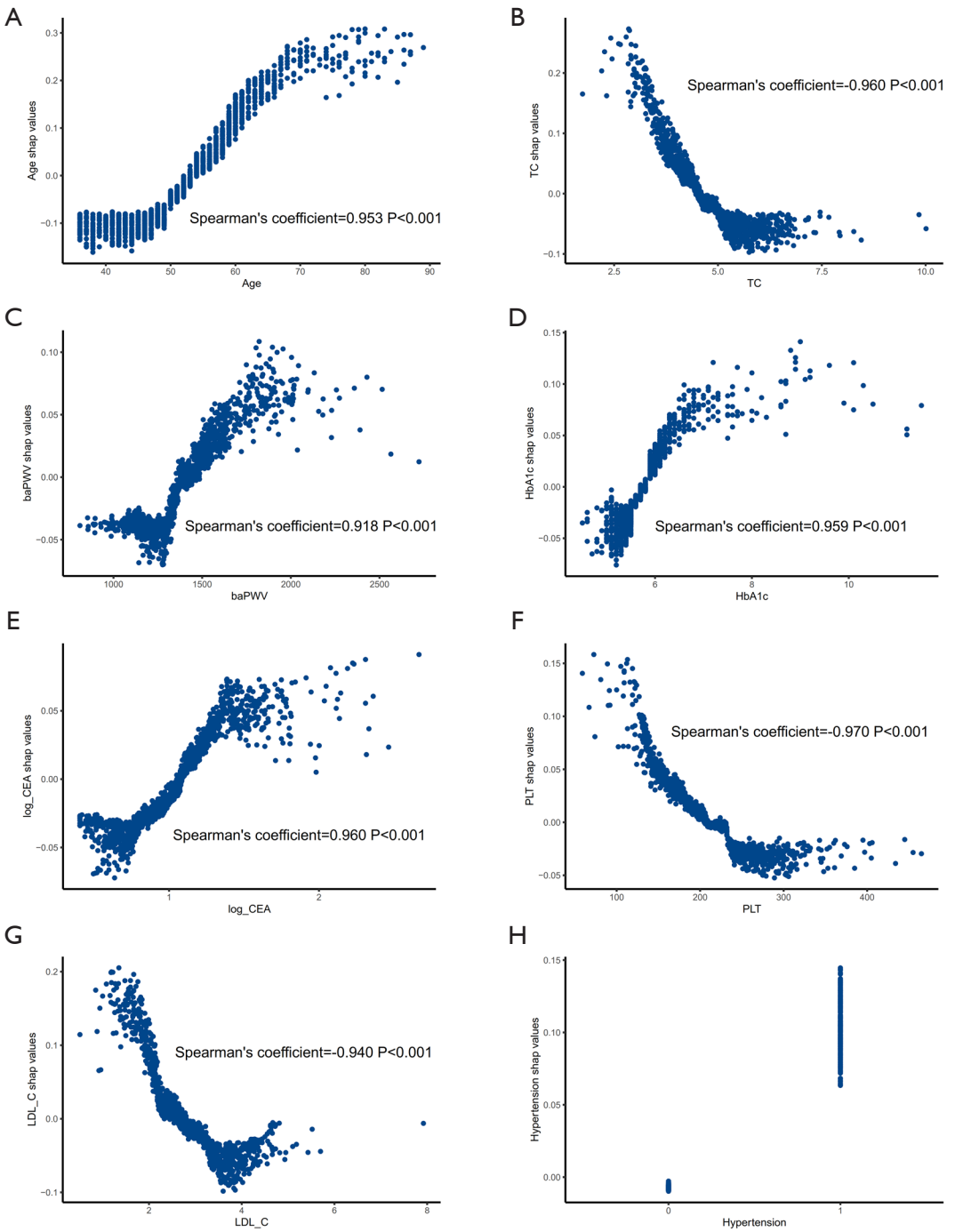

Figure S9 SHAP dependence plot of the coronary heart disease model. The x-axis represents the value of the feature. The y-axis shows the corresponding SHAP value, and represents the feature contribution on model output. (A-H) show the age, TC, baPWV, HbA1c, CEA, platelet count, LDL-C, and hypertension, respectively. TC, total cholesterol; baPWV, brachial-ankle pulse wave velocity; HbA1c, hemoglobin A1C; CEA, carcinoembryonic antigen; PLT, platelet; LDL-C, low-density lipoprotein cholesterol.

https://dx.doi.org/10.21037/atm-22-1916

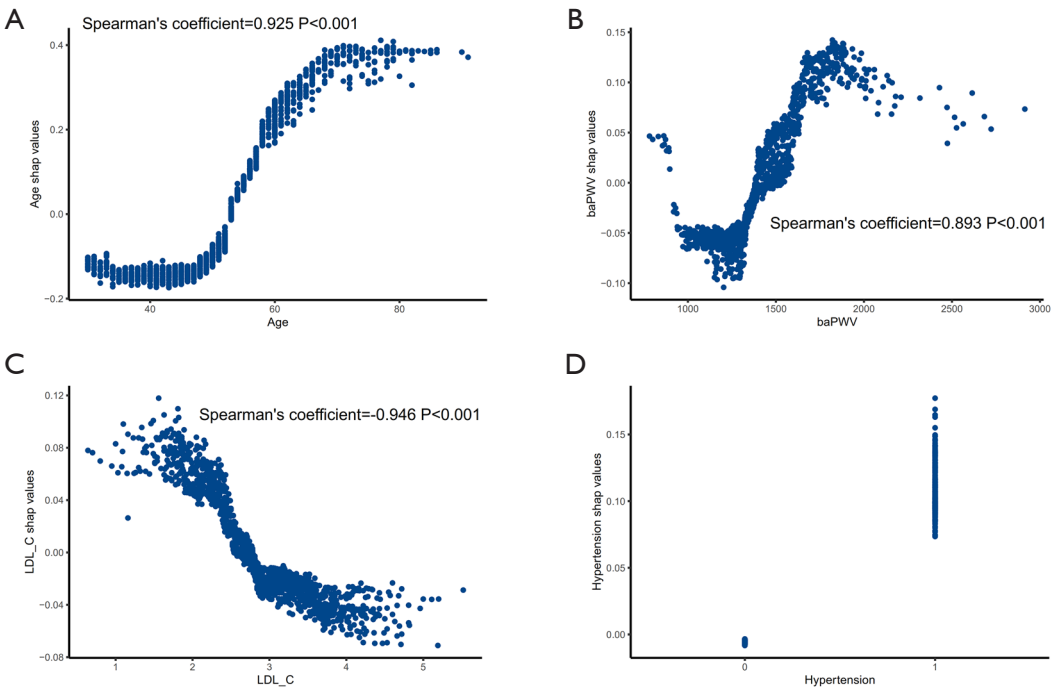

Figure S10 SHAP dependence plot of the ischemic stroke model. The x-axis represents the value of the feature. The y-axis shows the corresponding SHAP value, which represents the feature contribution on model output. (A-D) show the age, baPWV, LDL-C, and hypertension, respectively. baPWV, brachial-ankle pulse wave velocity; LDL-C, low-density lipoprotein cholesterol; SHAP, Shapley Additive exPlanations.

https://dx.doi.org/10.21037/atm-22-1916

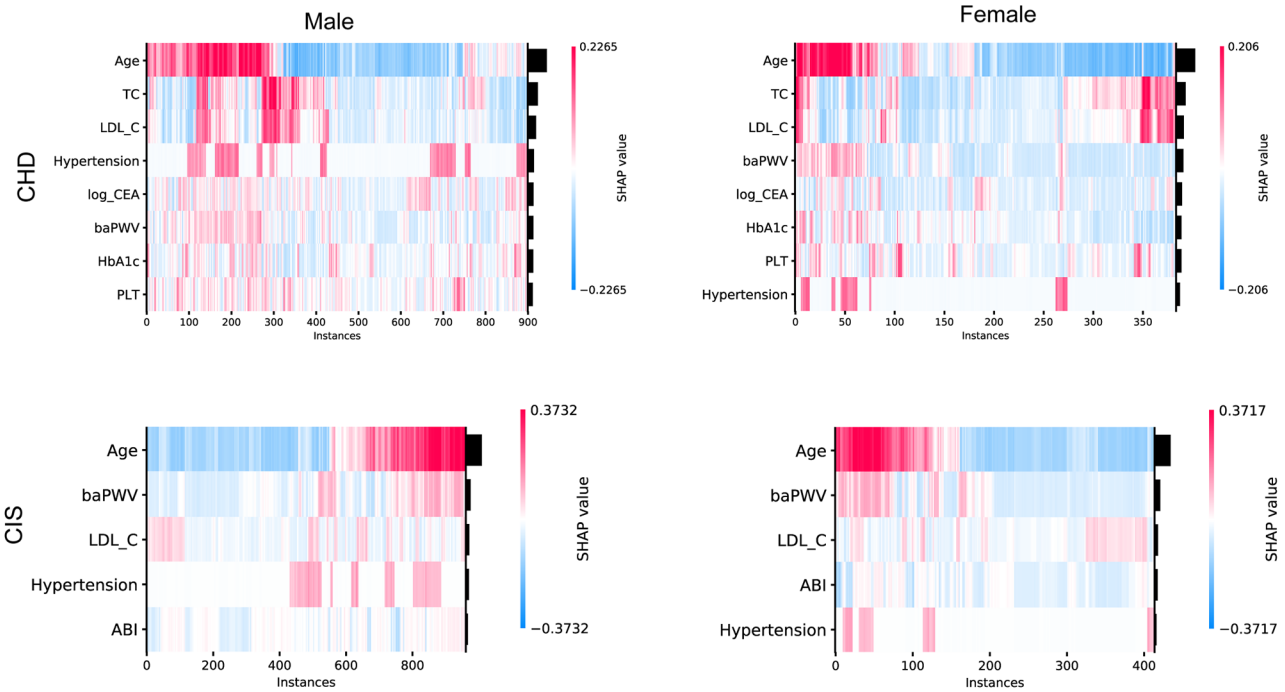

Figure S11 Analysis of gender differenced for features used in the models. CHD, coronary heart disease; CIS, cerebral ischemic stroke; TC, total cholesterol; LDL-C, low density lipoprotein cholesterol; CEA, carcinoembryonic antigen; baPWV, brachial-ankle pulse wave velocity; HbA1c, hemoglobin A1c; PLT, platelet; ABI, ankle-brachial index.

https://dx.doi.org/10.21037/atm-22-1916

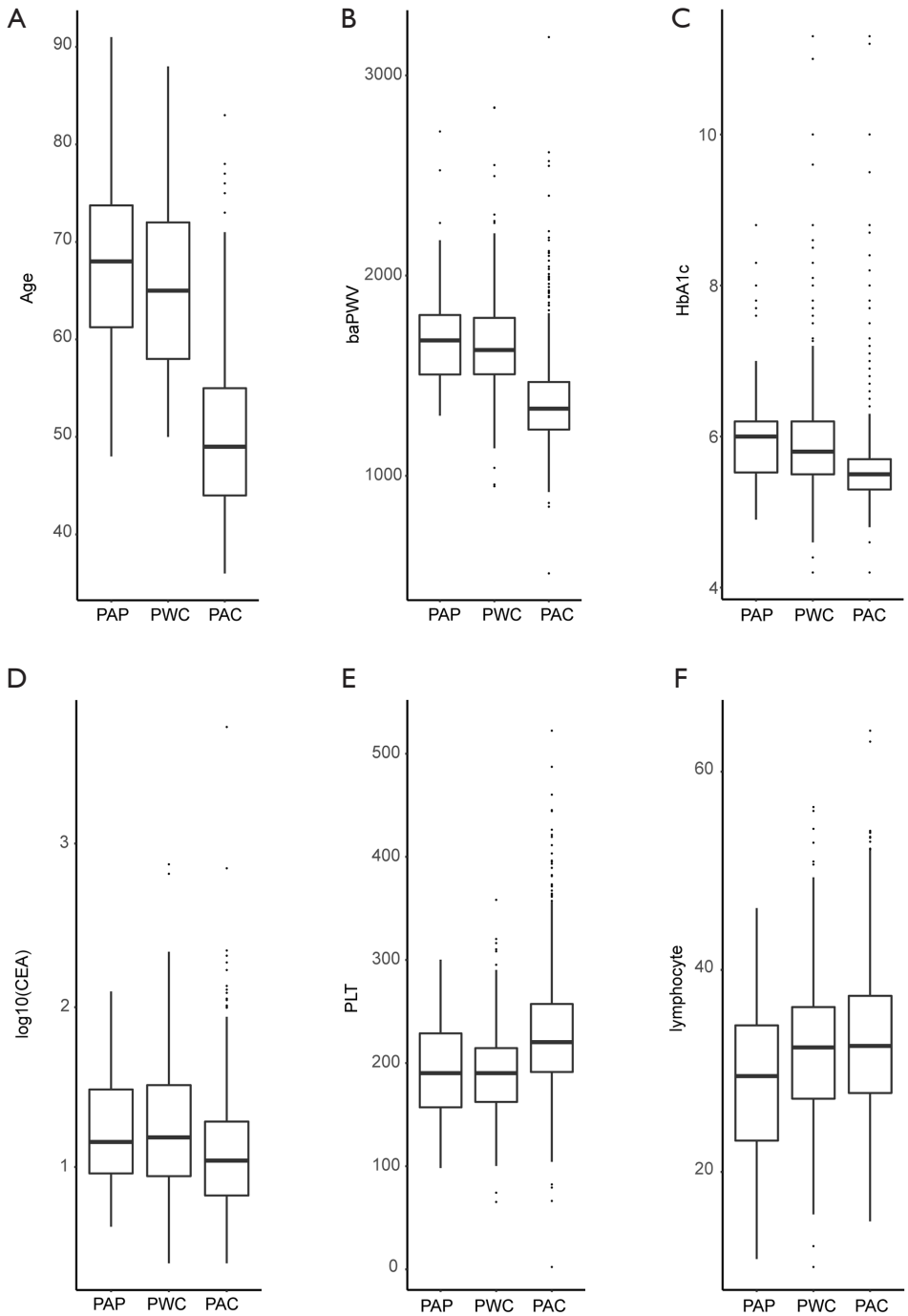

Figure S12 The dissimilarity characteristics between predicted accurate samples and predicted wrong controls in the coronary heart disease model. The y-axis represents characteristics, and (A-F) show the age, baPWV, HbA1c, CEA, platelet count, and percentage of lymphocytes, respectively. PAP, predicted accurate patients; PWC, predicted wrong controls; PAC, predicted accurate controls; baPWV, brachial-ankle pulse wave velocity; HbA1c, hemoglobin A1C; CEA, carcinoembryonic antigen; PLT, platelet.

https://dx.doi.org/10.21037/atm-22-1916

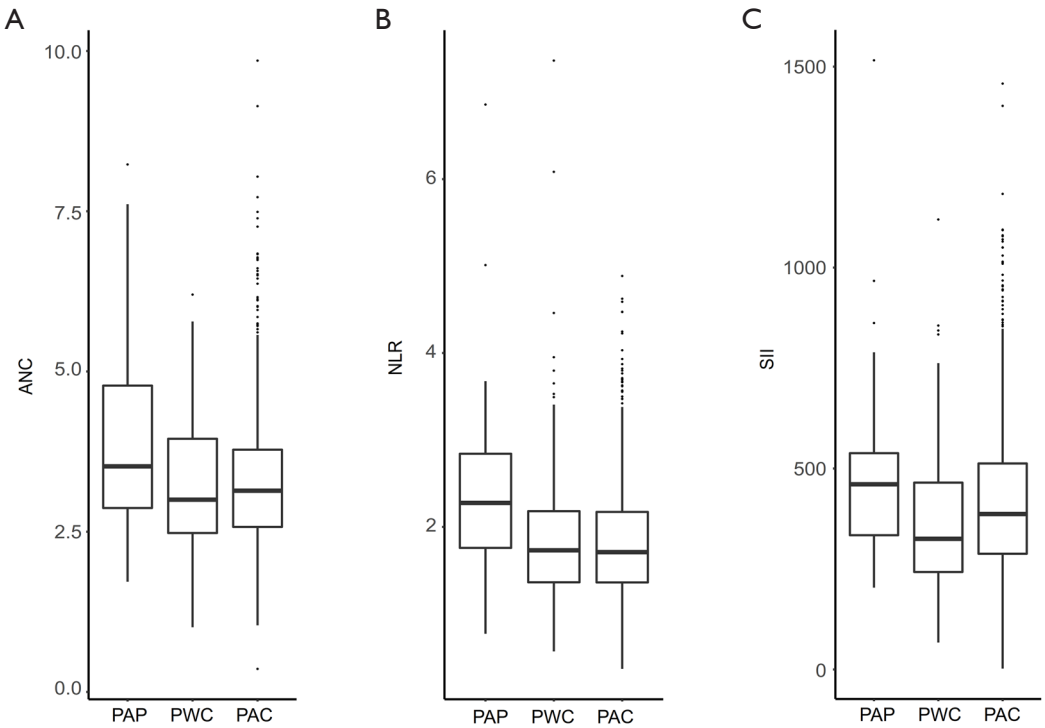

Figure S13 The value of inflammatory markers between predicted accurate samples and predicted wrong controls in the CHD model. The y-axis represents the characteristics, and (A-C) show the ANC, NLR, and SII, respectively. ANC, absolute neutrophil count; PAP, predicted accurate patients; PWC, predicted wrong controls; PAC, predicted accurate controls; NLR, neutrophil/lymphocyte ratio; SII, systemic immune inflammation index.

https://dx.doi.org/10.21037/atm-22-1916